Broadband Electro-Optic Traveling-Wave Light Modulators

By M. DiDOMENICO, JR. and L. K. ANDERSON

(Manuscript received June 13, 1963)

A detailed analysis has been carried out of a broadband traveling-wave electro-optic light modulator using single crystals of currently available materials. The structure analyzed is that first proposed by Rigrod and Kaminow in which a light beam is reflected back and forth across a microwave transmission line with the angle between optical and microwave phase velocity vectors chosen so that the component of the optical phase velocity vector in the direction of microwave propagation is equal to the microwave phase velocity. For generality both amplitude and phase modulation are considered in single crystals belonging to three different symmetry groups, T_d and $D_{2d}(V_d)$, (linear electro-optic effect) and O_h (quadratic effect), for two different orientations of the modulating field.

The inclusion of such practical factors as microwave and optical loss results in an optimum design in which the modulator dimensions and operating temperature are uniquely determined by the optical and microwave dielectric properties of the modulating medium. The main conclusions of the analysis are:

(i) Either cuprous chloride or suitably biased strontium titanate may be used to produce 50 per cent linear modulation over a bandwidth of 10 gc with less than 5 watts of modulating power, using structures a few centimeters long that have practical manufacturing and operating tolerances.

(ii) The upper modulation frequency limit is set by a cutoff frequency which arises from the finite width of the optical beam.

(iii) The presence of appreciable crystalline strain in the modulating medium requires that the modulating system consist of a simple phase modulator followed by some form of frequency-selective discriminator. Such a system requires monochromatic but not necessarily coherent light.

I. INTRODUCTION

Broadband microwave modulation of light requires the use of an extended traveling-wave structure. In order to obtain a cumulative inter-

action between the microwave and optical traveling waves, some form of velocity matching is necessary. In a structure of finite length a practical velocity matching criterion is that the component of the optical phase velocity vector taken along the microwave wave vector be equal to the microwave phase velocity. Several possible arrangements immediately suggest themselves for realizing this type of interaction. For example, we could use true traveling-wave structures[1-4] or iterative structures[5] where the optical and modulating signal are adjusted to interact intermittently with the proper phase. Broadband modulation further requires that the modulating structure have little dispersion, which implies propagation in a TEM or TEM-like mode. Thus, since the dielectric constants of usefully transparent modulating media are much less at optical frequencies than at microwave frequencies, broadband microwave modulation of light can be achieved by using some form of optical slow-wave structure, of which the simplest is that first proposed by Rigrod and Kaminow.[1] In this structure, shown schematically in Fig. 1, an optical plane wave zigzags back and forth in an electro-optic medium between plane mirrors while the interacting microwave modulating signal propagates longitudinally down the structure. The object of this paper is to analyze in detail the operating characteristics of this form of modulator, to present a systematic and quantitative procedure for designing modulators that require a minimum of modulating power, and finally to present numerical results for a number of presently available electro-optic materials.

The kinds of materials considered here fall into two classes. The first of these comprises materials which exhibit a linear electro-optic effect, and the second includes materials which possess a quadratic or Kerr electro-optic effect. The specific materials considered in the first class are:

(*i*) cubic crystals of symmetry T_d, such as cuprous chloride (CuCl) and zinc sulfide (ZnS),

(*ii*) KDP and its isomorphs of symmetry $D_{2d}(V_d)$.

The second class of materials consists of centrosymmetric cubic crystals of symmetry O_h such as the titanates ($SrTiO_3$ and $BaTiO_3$) operated in their paraelectric phase.

All electro-optic modulators using transparent media are basically phase modulators in that the modulating fields act directly to change the optical phase velocity of the medium. The phase modulation introduced on a light beam can then be used to transmit intelligence, or if desired it may be converted into intensity modulation. This latter process may in a sense be viewed as a homodyne process[6] in which we beat two phase-modulated normal modes of a birefringent modulating medium

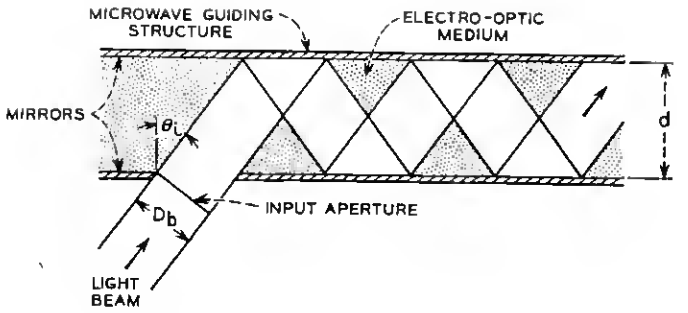

Fig. 1 — Basic zigzag modulator configuration (after Rigrod and Kaminow, Ref. 1).

(e.g., an ordinary and extraordinary wave), the mixing taking place in a polarization analyzer (e.g., a Nicol prism) following the modulator. Most amplitude modulators to date have been of this form.

A systematic comparison of the suitability of the aforementioned materials in a zigzag modulator is complicated by the fact that the optimum modulator configuration depends upon the form of modulation desired (e.g., AM, PM, polarization modulation, etc.) as well as on the demodulation system used (e.g., simple quantum counter, heterodyne, etc.). The comparison is further complicated by the necessity of taking into account such practical problems as crystalline strains, losses (both microwave and optical) and various operational and manufacturing tolerances. Of these effects the existence of strain, particularly random strain, is of paramount importance in determining the ultimate form the modulator will take. The effect of random strain is to partially destroy the spatial coherence of the modulated wave without affecting the temporal coherence. As a result the performance of any modulation-detection system which involves the mixing of two optical signals will be degraded, and we show in fact that the only system largely unaffected by strain is a phase modulator followed by an optical discriminator and quantum counter.

The organization of the remainder of the paper is as follows: In Section II we consider in general the basic phase modulation process in the zigzag modulator, obtaining expressions for the time-varying optical phase shifts which include the effects of microwave loss and lack of synchronism between optical and microwave signals. In Section III we use these results to obtain expressions for the modulation sensitivity of practical phase modulators. In Section IV the same thing is done for amplitude modulators. The practical implications of such effects as diffraction,

strain, optical losses, etc. are discussed in Section V. Finally, in Section VI we outline a procedure for selecting the optimum modulator dimensions and operating temperature so as to obtain the most efficient transfer of information onto the optical beam. In this same section we consider the question of modulator bandwidth.

We conclude with a tabulation of the performance to be expected from presently available materials in the zigzag modulator configuration. Our results show that it should be possible to build a modulator using either the quadratic effect in strontium titanate or the linear effect in cuprous chloride that will provide 50 per cent linear modulation over a 10 gc bandwidth for modulating powers less than about 5 watts. Two factors contribute to the high modulation sensitivity in strontium titanate. These are: (*i*) use of a dc bias results in a large effective microwave electro-optic coefficient, and (*ii*) a long optical path is obtained in a small volume of material, resulting in a very efficient use of microwave power.

II. GENERAL THEORY

The configuration analyzed is shown in Fig. 1. The light is assumed to propagate in the yz plane, between mirrors located in the xy plane, and to have its electric vector polarized either perpendicular to or parallel to the yz plane. The modulating wave propagates in the y direction, along the axis of the modulator.* We may distinguish two cases. In the first (see Fig. 2a) the electric vector of the modulating field lies in the optical plane of incidence (this we call the 0° modulator). In the second (see Fig. 2b) the modulating electric field is perpendicular to the optical plane of incidence (90° modulator). A TEM modulating wave can be propagated in the medium with either polarity if the mirrors are made of nonconducting dielectric multilayers.

In the presence of the modulating field and any dc bias, the optical index ellipsoid[7] is assumed to take the form shown in Fig. 3(a),† with the crystalline axes of the material aligned so that the principal axes of the ellipsoid coincide with the coordinate axes.‡ The significance of the

* For convenience, we choose to take the xz plane as the transverse plane of the modulator and the y axis as the direction of propagation or modulator axis. By aligning this Cartesian system with the principal axes of the index ellipsoid of the modulating medium, it can be shown that the only effect of changing the direction of propagation from, say, the y to the x axis is to cause a sign reversal in the retardation of the optical wave.

† By this assumption, we exclude cases in which the electro-optic effect takes the form of a field-dependent orientation of the index ellipsoid. It can be shown that this mode of operation is much less effective than the one in which the orientation of the index ellipsoid remains fixed, and only the lengths of the axes of the ellipsoid change.

‡ The crystal cut necessary to achieve this alignment for each material is given in Appendix A.

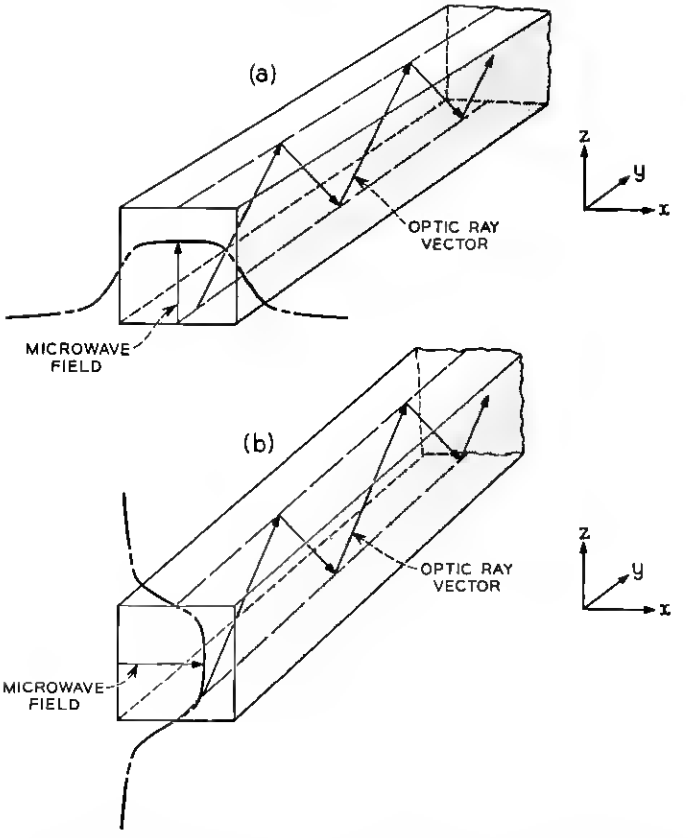

Fig. 2 — Relative orientation of modulating electric field and optical plane of incidence in the two zigzag modulator configurations: (a) 0° modulator; (b) 90° modulator.

index ellipsoid is that it defines the wave vectors and planes of polarization of the two normal modes which can propagate through the medium in any given direction. A plane perpendicular to the wave vector passing through the center of the ellipsoid cuts it in an ellipse whose major and minor axes define the directions of the two orthogonal planes of polarization. The lengths of these axes are equal to the reciprocals of the two indices of refraction. In the configuration shown in Fig. 1, the two normal modes have their electric vectors polarized respectively parallel and perpendicular to the plane of incidence. The two indices of refraction we denote by $n_\parallel$ and $n_\perp$; from Fig. 3(b) it is evident that

$$1/n_\perp^2 = 1/n_x^2 \tag{1a}$$

and

$$\frac{1}{n_{\parallel}^{\,2}} = \frac{\cos^2 \theta_i}{n_y^{\,2}} + \frac{\sin^2 \theta_i}{n_z^{\,2}}. \tag{1b}$$

As an optical plane wave traverses the modulating medium, its phase velocity varies continuously with time. A convenient way to deduce the time dependence of the over-all phase shift, and hence the phase modulation, is to follow the trajectory of a fixed point on the wave front as it moves through the medium. This is similar to the method of characteristics used to treat nonlinear and parametric wave propagation problems and is valid whenever the phase of the wave or the eikonal of geometrical

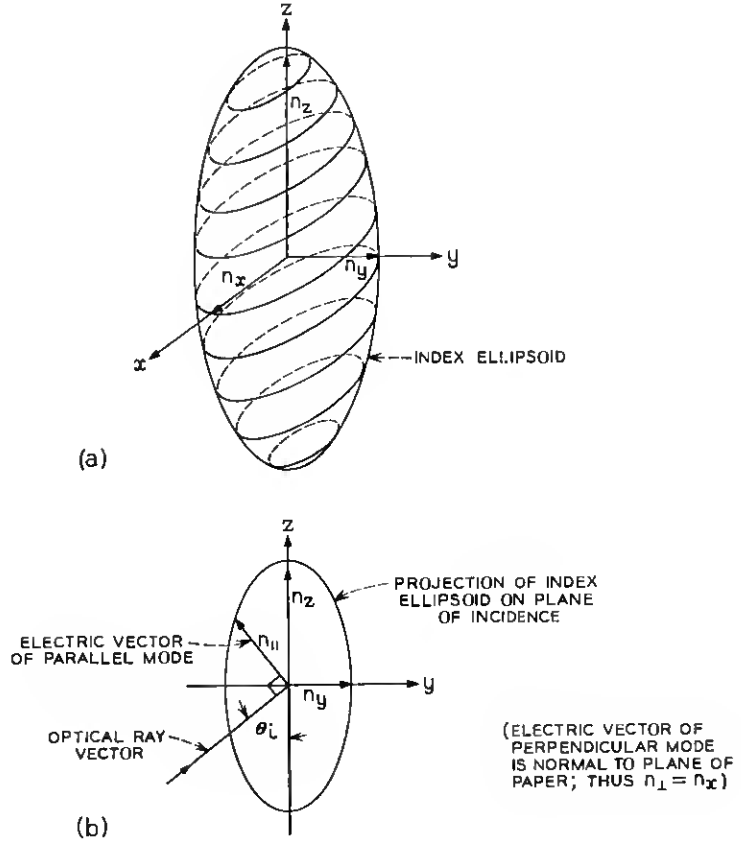

Fig. 3 — (a) Orientation of index ellipsoid with respect to coordinates of modulator; (b) projection of index ellipsoid on optical plane of incidence.

optics is large. When this condition is satisfied the wave propagates approximately as a plane wave. This can be demonstrated by expanding the eikonal in a power series over small space regions and time intervals.[8] It is then correct to say that the time taken for a point on the wavefront to advance a distance y along the modulator axis is given by

$$(t - t_0) = \frac{n_0 y}{c \sin \theta_i} \tag{2}$$

where c is the velocity of light in vacuo, n_0 is the refractive index in the absence of any electric field, t_0 is the starting time at $y = 0$, and θ_i is the angle between the light ray and the z axis. This simple expression replaces a complicated integral equation and is correct to first order in the fractional change $\Delta n/n$ in the index of refraction, and hence is valid only when $| \Delta n/n | \ll 1$, as is usually the case.

The value of the wave phase at any point in space is given by the integral

$$\varphi(t) = \omega \int_{\zeta_1}^{\zeta_2} \frac{d\zeta}{v_p(\zeta,t)}$$

where $\omega/2\pi$ is the optical frequency, and ζ is measured in the ray direction. This equation can be written in terms of the component of the phase velocity vector in the y-direction* as

$$\varphi(t) = \frac{\omega}{\sin \theta_i} \int_0^S \frac{dy}{v_p(y,t)} = \frac{2\pi}{\lambda_0 \sin \theta_i} \int_0^S n(y,t)\, dy \tag{3}$$

where λ_0 is the free-space optical wavelength and S the modulator length. Equation (3) applies separately to both normal modes of the electro-optic medium when the appropriate index of refraction n is used. How n depends on the applied electric field for the various materials and configurations of interest is derived in Appendix A.

By substituting (2) into (3) and utilizing the expressions derived in Appendix A for $n(y,t)$, one can calculate the time dependence of the wave phase correct to first order in the fractional change $\Delta n/n$. As long as the modulator length is bounded, as it must be if diffraction effects, etc., are to be minimized (see Section V), this calculation should give accurate results since $| \Delta n/n | \ll 1$.

In the remainder of this section we make use of (2) and (3) to obtain expressions for the wave phase as a function of time for the two normal modes of the modulating medium. These expressions describe the basic

* Note that when dispersion can be neglected the y component of the optical phase velocity vector is just the group velocity of the optical energy flow along the modulator axis.

modulation process within the medium. In subsequent sections we shall go on to describe the practical considerations involved in the actual realization of phase and amplitude modulators.

2.1 *Linear Electro-Optic Effect in Cubic Materials*

2.1.1 *0° Modulator*

For this case the two modes have refractive indices given by (1) and (104)

$$\frac{1}{n_\perp} = \frac{1}{n_0}(1 + n_0^2 r_{41} E_z)^{\frac{1}{2}} \tag{4}$$

$$\frac{1}{n_\parallel} = \frac{1}{n_0}(1 - n_0^2 r_{41} E_z \cos^2 \theta_i)^{\frac{1}{2}} \tag{5}$$

where r_{41} is the linear electro-optic coefficient (see Appendix A). For an attenuated modulating wave of the form

$$E_z(y,t) = E_m e^{-\alpha_m y} \cos(\omega_m t - \beta_m y) \tag{6}$$

the phase of the wave polarized perpendicular to the plane of incidence is approximately given by

$$\varphi_\perp(t_0) \approx \frac{2\pi}{\lambda_0} \frac{n_0}{\sin \theta_i} \int_0^S \{1 - \tfrac{1}{2} n_0^2 r_{41} E_m e^{-\alpha_m y} \cos[\omega_m t_0 + (\beta_e - \beta_m) y]\}\, dy \tag{7}$$

where for convenience we have introduced the notation

$$\frac{n_0 \omega_m}{c \sin \theta_i} \equiv \beta_e . \tag{8}$$

The approximation holds when $| n_0^2 r_{41} E_m | \ll 1$. Equation (7) can be integrated directly, giving

$$\varphi_\perp(t) = \frac{2\pi}{\lambda_0} \frac{n_0}{\sin \theta_i} S - \frac{2\pi}{\lambda_0} \frac{n_0^3}{\sin \theta_i} r_{41} E_m e^{-\alpha_m S/2} \times \left(\frac{\sinh^2 \frac{\alpha_m S}{2} + \sin^2 \frac{\beta S}{2}}{\alpha_m^2 + \beta^2} \right)^{\frac{1}{2}} \cos(\omega_m t + \psi) \tag{9}$$

where β is defined by

$$\beta = \beta_e - \beta_m \tag{10}$$

and ψ is a time-independent phase factor. In the absence of microwave losses this reduces to the result obtained earlier by Kaminow and Liu.[2] It is evident that the phase modulation described by (9) is maximized by the choice $\beta = \beta_e - \beta_m = 0$, corresponding to the matching of the y-components of the microwave and optical phase velocity vectors. Thus, it is clear that microwave losses do not affect the basic velocity matching condition. Under this condition (9) reduces to

$$\varphi_\perp(t) = \frac{2\pi}{\lambda_0} \frac{n_0 S}{\sin \theta_i} [1 - \tfrac{1}{2} n_0^2 r_{41} E_m f(\alpha_m S/2) \cos \omega_m t] \tag{11}$$

where for the sake of brevity we have defined the function $f(\alpha_m S/2)$ by

$$\exp\left(-\frac{\alpha_m S}{2}\right)\left[\frac{\sinh(\alpha_m S/2)}{(\alpha_m S/2)}\right] \equiv f\left(\frac{\alpha_m S}{2}\right). \tag{12}$$

For the other wave, whose plane of polarization lies in the plane of incidence, the corresponding expression is

$$\varphi_\parallel(t) = \frac{2\pi}{\lambda_0} \frac{n_0 S}{\sin \theta_i}\left[1 + \tfrac{1}{2} n_0^2 r_{41} E_m \cos^2 \theta_i f\left(\frac{\alpha_m S}{2}\right) \cos \omega_m t\right]. \tag{13}$$

2.1.2 *90° Modulator*

The analysis for the 90° modulator is formally identical, except that (105) is used for the principal indices of refraction, in place of (104), so that

$$1/n_\perp = 1/n_0 \tag{14a}$$

and

$$\frac{1}{n_\parallel} = \frac{1}{n_0}(1 - n_0^2 r_{41} E_x \cos 2\theta_i)^{\frac{1}{2}}. \tag{14b}$$

The results for a modulating wave of the form given by (6) are

$$\varphi_\perp(t) = \frac{2\pi}{\lambda_0} \frac{n_0 S}{\sin \theta_i} = \text{constant} \tag{15}$$

and

$$\varphi_\parallel(t) = \frac{2\pi}{\lambda_0} \frac{n_0 S}{\sin \theta_i}\left[1 + \tfrac{1}{2} n_0^2 r_{41} E_m \cos 2\theta_i f\left(\frac{\alpha_m S}{2}\right) \cos \omega_m t\right]. \tag{16}$$

2.2 *Quadratic Electro-Optic Effect in Cubic and/or Amorphous Materials*

The analysis for the quadratic effect in the presence of a large dc bias is very similar to that for the linear effect. The situation is complicated

somewhat by the presence of two independent electro-optic coefficients in the case of the quadratic effect in cubic crystals (see Appendix A). We consider the two configurations discussed before, in which the modulating field lies parallel (0° modulator) or perpendicular (90° modulator) to the optical plane of incidence.

2.2.1 *0° Modulator*

For this case the relevant refractive indices are [refer to (110)]

$$\frac{1}{n_\perp} = \frac{1}{n_0}(1 + n_0^2\rho_2 E_z^2)^{\frac{1}{2}} \tag{17}$$

and

$$\frac{1}{n_\parallel} = \frac{1}{n_0}\left[1 + n_0^2\rho_1 E_z^2\left(\sin^2\theta_i + \frac{\rho_2}{\rho_1}\cos^2\theta_i\right)\right]^{\frac{1}{2}} \tag{18}$$

where ρ_1 and ρ_2 are quadratic electro-optic coefficients (see Appendix A). In order to achieve approximately linear modulation, as well as to enhance the modulation sensitivity, the applied field should consist of a large static bias and a smaller microwave field, so that

$$E_z(y,t) = E_0 + E_m e^{-\alpha_m y}\cos(\omega_m t - \beta_m y). \tag{19}$$

Then to first order in E_m/E_0

$$E_z^2 \approx E_0^2 + 2E_0E_m e^{-\alpha_m y}\cos(\omega_m t - \beta_m y)$$

and the expressions for $1/n_\perp$ and $1/n_\parallel$ become linear in E_m. The integrations needed to obtain $\varphi_\perp$ and $\varphi_\parallel$ are similar to those in the preceding section. Again the maximum ac phase shift occurs with velocity matching, for which case we obtain

$$\varphi_\perp(t) = \frac{2\pi}{\lambda_0}\frac{n_0 S}{\sin\theta_i}\left\{1 - \tfrac{1}{2}n_0^2\rho_2 E_0\left[E_0 + 2E_m f\left(\frac{\alpha_m S}{2}\right)\cos\omega_m t\right]\right\} \tag{20}$$

and

$$\begin{aligned}\varphi_\parallel(t) = \frac{2\pi}{\lambda_0}\frac{n_0 S}{\sin\theta_i}\Bigg\{1 - \tfrac{1}{2}n_0^2\rho_1 E_0\left(\sin^2\theta_i + \frac{\rho_2}{\rho_1}\cos^2\theta_i\right)\\ \times\left[E_0 + 2E_m f\left(\frac{\alpha_m S}{2}\right)\cos\omega_m t\right]\Bigg\}.\end{aligned} \tag{21}$$

In deriving (20) and (21) we note that because the dc bias makes the material birefringent even in the absence of a microwave modulating field, the ordinary ($\perp$) and extraordinary ($\parallel$) modes cannot, strictly

speaking, be simultaneously matched to the modulating wave. We assume, however, that the bias is small ($|\, n_0^2 \rho E_0^2 \,| \ll 1$) so that the distinction between ordinary and extraordinary phase velocities becomes unimportant. For known materials this condition is met for fields as large as 10^5 v/cm — i.e., for any field that the material can sustain without dielectric breakdown.

2.2.2 *90° Modulator*

The analysis here is similar to the 0° case, except that the indices of refraction are simply [refer to (111)]

$$\frac{1}{n_\perp} = \frac{1}{n_0}(1 + n_0^2 \rho_1 E_x^2)^{\frac{1}{2}} \tag{22a}$$

and

$$\frac{1}{n_\parallel} = \frac{1}{n_0}(1 + n_0^2 \rho_2 E_x^2)^{\frac{1}{2}} \tag{22b}$$

so that the resulting wave phases are

$$\varphi_\perp(t) = \frac{2\pi}{\lambda_0}\frac{n_0 S}{\sin\theta_i}\left\{1 - \tfrac{1}{2} n_0^2 \rho_1 E_0 \left[E_0 + 2E_m f\left(\frac{\alpha_m S}{2}\right)\cos\omega_m t\right]\right\} \tag{23}$$

and

$$\varphi_\parallel(t) = \frac{2\pi}{\lambda_0}\frac{n_0 S}{\sin\theta_i}\left\{1 - \tfrac{1}{2} n_0^2 \rho_2 E_0 \left[E_0 + 2E_m f\left(\frac{\alpha_m S}{2}\right)\cos\omega_m t\right]\right\}. \tag{24}$$

2.3 *Linear Electro-Optic Effect in Uniaxial Materials*

The results here are similar to those obtained earlier for the effect in cubic materials.

2.3.1 *0° Modulator*

Equations (1) and (113) apply here, so that

$$\begin{aligned} \frac{1}{n_\perp} &= \frac{1}{n_0}(1 + n_0^2 r_{63} E_z)^{\frac{1}{2}} \\ \frac{1}{n_\parallel} &\approx \frac{1}{n_0}\left(1 - n_0^2 r_{63} E_z \cos^2\theta_i - \frac{2\Delta n}{n_0}\sin^2\theta_i\right)^{\frac{1}{2}} \end{aligned} \tag{25}$$

where we have set $\Delta n \equiv n_e - n_0$, which we assume to be much less than unity (n_e refers to the extraordinary refractive index). The wave phases for the two modes are then given by

$$\varphi_{\perp}(t) = \frac{2\pi}{\lambda_0}\frac{n_0 S}{\sin\theta_i}\left[1 + \tfrac{1}{2}n_0^2 r_{63}E_m f\left(\frac{\alpha_m S}{2}\right)\cos\omega_m t\right] \tag{26}$$

and

$$\varphi_{\parallel}(t) = \frac{2\pi}{\lambda_0}\frac{n_0 S}{\sin\theta_i} \times\left[1 - \frac{2\Delta n}{n_0}\sin^2\theta_i - \tfrac{1}{2}n_0^2 r_{63}E_m\cos^2\theta_i f\left(\frac{\alpha_m S}{2}\right)\cos\omega_m t\right]. \tag{27}$$

2.3.2 *90° Modulator*

From (1) and (114) we obtain

$$1/n_{\perp} = 1/n_e$$

and

$$\frac{1}{n_{\parallel}} = \frac{1}{n_0}(1 - n_0^2 r_{63}E_x\cos^2\theta_i)^{\frac{1}{2}} \tag{28}$$

so that the wave phases are

$$\varphi_{\perp}(t) = \frac{2\pi}{\lambda_0}\frac{n_e S}{\sin\theta_i} = \text{constant} \tag{29}$$

and

$$\varphi_{\parallel}(t) = \frac{2\pi}{\lambda_0}\frac{n_0 S}{\sin\theta_i}\left[1 - \tfrac{1}{2}n_0^2 r_{63}E_m\cos 2\theta_i f\left(\frac{\alpha_m S}{2}\right)\cos\omega_m t\right]. \tag{30}$$

III. PHASE MODULATORS

The preceding results are immediately applicable to the phase modulator. The maximum modulation sensitivity is obtained when the beam is linearly polarized in the direction ($\perp$ or $\parallel$) showing the greatest effect, although unpolarized light can also be used.

For all the cases discussed in the previous section, the ac component of the wave phase can be written in the form

$$\varphi_{ac}(t) = \frac{2\pi n_0^3}{\lambda_0} ASg(\theta_i) f\left(\frac{\alpha_m S}{2}\right) E_m\cos\omega_m t, \tag{31}$$

where A is proportional to electro-optic coefficient and $g(\theta_i)$ depends on the angle of incidence. The quantity of most immediate interest is the modulation sensitivity, which we may define as the ratio of the

peak phase shift to the square root of the power input to the modulator.* To make the problem definite, we consider a parallel-plate line of spacing h and width w, filled with a medium of microwave dielectric constant κ'. If we ignore fringing fields,† the power flow is given in terms of the electric field by

$$P = \frac{1}{2}\frac{\sqrt{\kappa'}}{\eta} E_m^2 hw, \tag{32}$$

where $\eta = 377$ ohms is the impedance of free space. The modulation sensitivity is then

$$\left|\frac{M}{\sqrt{P}}\right| = \frac{2\pi n_0^3}{\lambda_0} ASg(\theta_i) f\left(\frac{\alpha_m S}{2}\right)\sqrt{\frac{2\eta}{\sqrt{\kappa'}\, hw}} \tag{33}$$

where M is the peak ac phase shift. Since the angle of incidence is determined in terms of material parameters by the velocity matching condition $\beta_e = \beta_m$, which reduces to $\sin\theta_i = n_0/\sqrt{\kappa'}$ for the present geometry, (33) can also be written as

$$\left|\frac{M}{\sqrt{P}}\right| = \frac{2\pi n_0^3}{\lambda_0} ASp\left(\frac{n_0}{\sqrt{\kappa'}}\right) f\left(\frac{\alpha_m S}{2}\right)\sqrt{\frac{2\eta}{\sqrt{\kappa'}\, hw}} \tag{34}$$

where $p(n_0/\sqrt{\kappa'})$ is a function of $(n_0/\sqrt{\kappa'})$ which replaces $g(\theta_i)$. Values of A, $g(\theta_i)$ and $p(n_0/\sqrt{\kappa'})$ for the cases of interest here are given in Table I. In this table, the linear electro-optic coefficient which we write simply as r_{ij} is to be taken to be r_{41} in the case of cubic materials, and r_{63} for uniaxial crystals.

Numerical results for the power required in practical cases are given in Section VII.

IV. AMPLITUDE MODULATORS

In this section we treat the problem of obtaining broadband amplitude-modulated light by suitably combining the two simultaneously phase-modulated normal modes of a transparent electro-optic medium. In the ensuing treatment we will consider only the intensity variations in the modulated beam. In so doing we are ignoring the phase information that would be recovered, for example, by an optical heterodyne re-

* The advantage of defining a modulation sensitivity in this way is that it is a function of the microwave-optical properties of the electro-optic modulating medium and is expressed in terms of power which is easily measured.

† The effects of fringing fields and the problems associated with non-TEM mode propagation in this structure are considered in Section 5.1.

TABLE I — FUNCTIONS APPEARING IN (33) AND (34) FOR VARIOUS PHASE MODULATOR CONFIGURATIONS

Modulator	Mode	A	$g(\theta_i)$	$p(n_0/\sqrt{\kappa'})$
Linear, 0°	$\perp$	$\frac{1}{2}r_{ij}$	$1/\sin\theta_i$	$\sqrt{\kappa'}/n_0$
	$\parallel$	$\frac{1}{2}r_{ij}$	$\dfrac{\cos^2\theta_i}{\sin\theta_i}$	$\dfrac{\sqrt{\kappa'}}{n_0}\left(1-\dfrac{n_0^2}{\kappa'}\right)$
Linear, 90°	$\perp$	0	—	—
	$\parallel$	$\frac{1}{2}r_{ij}$	$\dfrac{\cos 2\theta_i}{\sin\theta_i}$	$\dfrac{\sqrt{\kappa'}}{n_0}\left(1-\dfrac{2n_0^2}{\kappa'}\right)$
Quadratic, 0°	$\perp$	$\rho_2 E_0$	$1/\sin\theta_i$	$\sqrt{\kappa'}/n_0$
	$\parallel$	$\rho_1 E_0$	$\dfrac{\sin^2\theta_i+\dfrac{\rho_2}{\rho_1}\cos^2\theta_i}{\sin\theta_i}$	$\dfrac{\dfrac{n_0^2}{\kappa'}+\dfrac{\rho_2}{\rho_1}\left(1-\dfrac{n_0^2}{\kappa'}\right)}{\dfrac{n_0}{\sqrt{\kappa'}}}$
Quadratic, 90°	$\perp$ $\parallel$	$\rho_1 E_0$ $\rho_2 E_0$	$1/\sin\theta_i$	$\sqrt{\kappa'}/n_0$

ceiver, and in effect are assuming that the receiver is a simple quantum counter. Thus we look for modulation of the form

$$I(t) = I_0(1 + M\cos\omega_m t) \tag{35}$$

where I_0 is the average light intensity and M is the modulation index.

Cubic materials are of particular interest as amplitude modulators since they are isotropic in the absence of an applied field and become uniaxial only upon application of a field. This is in contrast to what takes place in materials with lower degrees of symmetry where naturally occurring birefringence exists. The significance of starting with an isotropic crystal, as opposed to a uniaxial or even biaxial crystal, is that in the former no static retardation is accumulated between the two normal modes. Hence any ac difference in phase produced between these modes can easily be converted into useful intensity modulation. The presence of a static contribution to the differential phase shift can cause the induced ac birefringence to be masked out due to the angular spread of the beam, constructional uncertainties or finite source linewidth. (See Section 4.3.)

There are two simple ways in which a time-varying phase shift be-

tween two orthogonally polarized light beams may be converted into approximately linear intensity modulation. One of these is most useful when there is no dc retardation between the two beams, and the other when there is a controllable dc retardation, as in the biased quadratic effect modulator.

4.1 *Amplitude Modulation Using the Linear Electro-Optic Effect in Cubic Materials*

The first method of producing amplitude modulation is shown in Fig. 4. Circularly polarized light is produced by passing the linearly polarized incident beam through a quarter-wave plate in the manner shown.

The light emerging from the quarter-wave plate may be decomposed into two orthogonal normal modes, one aligned with the fast or ζ axis of the quarter-wave plate and the other aligned with the slow or ξ axis (see Fig. 4). Both normal modes are of equal amplitude but separated in phase by 90°. In order to obtain the desired modulation, the plane of transmission of the analyzer must make an angle of 45° with the plane of incidence.

For the arrangement given in Fig. 4 one can easily show that the ratio of transmitted to incident light intensity is given by

$$I_t/I_0 = \tfrac{1}{2}[1 + \sin(\varphi_\perp - \varphi_\parallel)]. \tag{36}$$

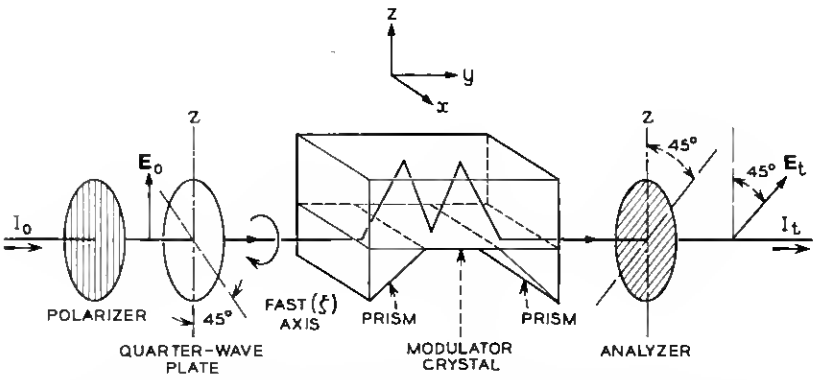

Fig. 4 — Arrangement for obtaining linear amplitude modulation for cubic crystals exhibiting a linear electro-optic effect. This arrangement can also be used with uniaxial crystals if the quarter-wave plate is replaced by a suitable optical compensator.

For the modulators using the linear electro-optic effect in cubic crystals, (11), (13), (15), and (16) yield

$$\varphi_\perp - \varphi_\parallel = -\frac{\pi n_0^3 r_{41}}{\lambda_0} E_m S g(\theta_i) f\left(\frac{\alpha_m S}{2}\right) \cos \omega_m t \tag{37}$$

where

$$g(\theta_i) = \begin{cases} \dfrac{1 + \cos^2 \theta_i}{\sin \theta_i} & (0° \text{ modulator}) \\ \dfrac{\cos 2\theta_i}{\sin \theta_i} & (90° \text{ modulator}). \end{cases} \tag{38}$$

To obtain a specific expression for the modulation sensitivity, which we define as $|M/\sqrt{P}|$ as before, we may again consider the simple parallel plate geometry discussed in Section III. It is evident from (36) and (37) that the modulated signal will in general consist of an infinite number of sidebands whose amplitudes are determined by Bessel functions. For simplicity we limit ourselves to the case of small modulation index (viz., $|\varphi_\perp - \varphi_\parallel| < \pi/6$) so that only the first sideband is important. We then obtain for the modulation sensitivity

$$\left|\frac{M}{\sqrt{P}}\right| = \frac{\pi\sqrt{\eta/2}}{V_{\frac{1}{2}}} \frac{S}{\sqrt{hw}} \frac{1}{\kappa'^{\frac{1}{4}}} p\left(\frac{n_0}{\sqrt{\kappa'}}\right) f\left(\frac{\alpha_m S}{2}\right), \tag{39}$$

with

$$p\left(\frac{n_0}{\sqrt{\kappa'}}\right) = \begin{cases} \dfrac{2 - n_0^2/\kappa'}{n_0/\sqrt{\kappa'}} & (0° \text{ modulator}) \\ \dfrac{1 - 2n_0^2/\kappa'}{n_0/\sqrt{\kappa'}} & (90° \text{ modulator}). \end{cases} \tag{40}$$

In this expression we have again used the velocity matching condition $\sin \theta_i = n_0/\sqrt{\kappa'}$ to replace $g(\theta_i)$ by $p(n_0/\sqrt{\kappa'})$, and have replaced the electro-optic coefficient with the more generally useful half-wave retardation voltage, $V_{\frac{1}{2}}$, defined by*

$$V_{\frac{1}{2}} = \frac{\lambda_0}{2n_0^3 r_{41}}. \tag{41}$$

Once again we defer computing actual numbers until Section VII.

* Note that when applied to the transverse electro-optic effect $V_{\frac{1}{2}}$ need not be the actual voltage applied to the crystal to obtain π phase retardation, which depends on the geometry of the crystal, but is to be viewed as a convenient collection of constants.

4.2 *Amplitude Modulation Using the Quadratic Electro-Optic Effect*

Use of the quadratic effect in conjunction with a dc bias to provide amplitude modulation differs from the linear case just considered in that there is now a bias-field dependent static phase difference produced between the ordinary and extraordinary rays. Approximately linear intensity modulation can be obtained in this case by placing the active medium between crossed polarizer and analyzer, as shown in Fig. 5, provided that the dc bias is adjusted so that operation occurs about the point of half-transmission. For the arrangement of Fig. 5, the ratio of transmitted to incident light intensity is given by

$$I_t/I_0 = \tfrac{1}{2}[1 + \cos(\varphi_\perp - \varphi_\parallel)]. \tag{42}$$

According to (20), (21), (23), and (24), the phase difference for the quadratic effect can be written as

$$|\varphi_\perp - \varphi_\parallel| = \frac{\pi n_0^3}{\lambda_0}(\rho_1 - \rho_2)E_0 S g(\theta_i)\left[E_0 + 2E_m f\left(\frac{\alpha_m S}{2}\right)\cos \omega_m t\right] \tag{43}$$

where

$$g(\theta_i) = \begin{cases} \sin \theta_i & (0^\circ \text{ modulator}) \\ 1/\sin \theta_i & (90^\circ \text{ modulator}). \end{cases} \tag{44}$$

Equation (43) is in the form $\varphi_\perp - \varphi_\parallel = \gamma_{dc} + \gamma_{ac}$; hence (42) can be written:

$$I_t/I_0 = \tfrac{1}{2}[1 + \cos \gamma_{dc} \cos \gamma_{ac} - \sin \gamma_{dc} \sin \gamma_{ac}]. \tag{45}$$

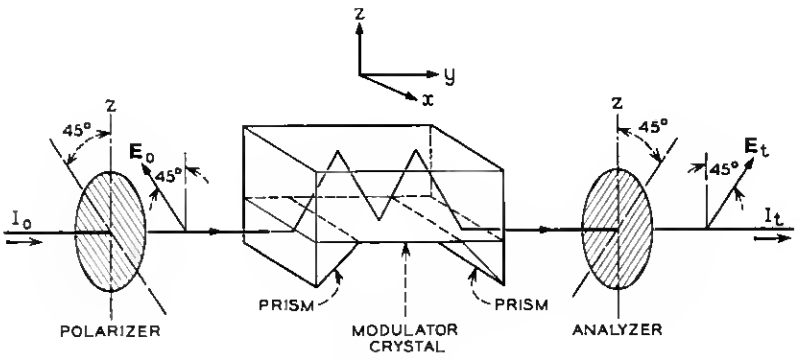

Fig. 5 — Arrangement for obtaining linear amplitude modulation in materials exhibiting a quadratic electro-optic effect.

For $\gamma_{ac} < \pi/6$ (small modulation) this becomes, approximately

$$I_t/I_0 \approx \tfrac{1}{2}(1 - \gamma_{ac} \sin \gamma_{dc}). \tag{46}$$

Maximum modulation sensitivity results when the operating point is chosen so that*

$$\gamma_{dc} \equiv \frac{\pi n_0^3(\rho_1 - \rho_2)E_0^2 S g(\theta_i)}{\lambda_0} = (2m + 1)\frac{\pi}{2}, \qquad m = 0, 1, 2, \cdots. \tag{47}$$

The point that should be noted here is that for the linear Kerr effect modulator there are modes of operation and that these modes, which are designated by the index m, constitute an independent operating variable.

For the operating points defined by (47), the modulation sensitivity for the parallel-plate geometry can be written in the form

$$\left|\frac{M}{\sqrt{P}}\right| = 4\pi\sqrt{2\eta}\,\frac{S}{\sqrt{hw}}\,\frac{1}{\kappa'^{\frac{1}{4}}}\,p\left(\frac{n_0}{\sqrt{\kappa'}}\right)KE_0 f\left(\frac{\alpha_m S}{2}\right), \tag{48}$$

where

$$p\left(\frac{n_0}{\sqrt{\kappa'}}\right) = \begin{cases} \dfrac{n_0}{\sqrt{\kappa'}} & (0° \text{ modulator}) \\ \dfrac{\sqrt{\kappa'}}{n_0} & (90° \text{ modulator}). \end{cases} \tag{49}$$

In deriving this equation we have, as before, made use of the synchronism condition $\sin \theta_i = n_0/\sqrt{\kappa'}$, and have replaced the electro-optic coefficient $(\rho_1 - \rho_2)$ by the more familiar Kerr constant

$$K = \frac{n_0^3(\rho_1 - \rho_2)}{2\lambda_0}. \tag{50}$$

It should be noted that the dc field is not an independent variable, but, because it determines the operating point [see (47)], is limited to the discrete values

$$E_0 = \frac{1}{2}\sqrt{\frac{(2m + 1)}{KSp\left(\dfrac{n_0}{\sqrt{\kappa'}}\right)}}. \tag{51}$$

In practice E_0 would be made as large as the dielectric strength of the material would permit, subject to (50). We should point out that the

* It is obvious that the arrangement shown in Fig. 4 could also be utilized here if desired; the only difference would be that the quiescent operating point would be chosen to make the dc part of $\varphi_\perp - \varphi_\parallel$ in (43) an odd multiple of π.

effects of electrostriction at high dc fields will undoubtedly result in electrostrictively induced birefringence. To the extent that the electrostriction is uniform, it is equivalent to a change in the Kerr constant, and can be compensated for by tuning E_0. On the other hand, nonuniform electrostriction can degrade the modulator performance in the same way as nonuniform strain. (See Section 5.6.)

4.3 *Amplitude Modulation Using the Transverse Linear Electro-Optic Effect in Uniaxial Crystals*

Use of the zigzag configuration to produce amplitude modulation with noncubic materials is complicated somewhat by the presence of a large static phase retardation due to the natural birefringence of the material. When the modulator is used with well-collimated monochromatic light, however, the effects of the natural birefringence can in principle be eliminated by means of an optical compensator, thereby making it worthwhile to consider this case as well.

The physical arrangement used in conjunction with the linear effect in cubic crystals, and shown in Fig. 4, is also applicable here if we replace the quarter-wave plate by a suitable compensator.[10] The compensator allows the phase of one optical mode of the modulator to be varied relative to that of the other.

For this arrangement the ratio of transmitted to incident intensity is given by

$$I_t/I_0 = \tfrac{1}{2}[1 + \cos(\varphi_\perp - \varphi_\parallel + \varphi_c)] \tag{52}$$

where φ_c is the relative phase shift introduced by the compensator. The phase retardation in the modulator is given by (26) to (30), and has the form

$$\varphi_\perp - \varphi_\parallel = -\frac{\pi n_0^3 r_{63}}{\lambda_0} E_m S g(\theta_i) f\left(\frac{\alpha_m S}{2}\right) \cos(\omega_m t) + \varphi_s \tag{53}$$

where $g(\theta_i)$ is given by (38) of Section 4.2 and φ_s is the static retardation, given by

$$\varphi_s = \begin{cases} \dfrac{4\pi \Delta n S}{\lambda_0} \sin\theta_i & (0^\circ \text{ modulator}) \\ 2\pi \dfrac{\Delta n S}{\lambda_0} \dfrac{1}{\sin\theta_i} & (90^\circ \text{ modulator}). \end{cases} \tag{54}$$

It is evident from (52) and (53) that maximum linear amplitude modulation is obtained when the compensator phase shift is adjusted so that

$$\varphi_c + \varphi_s = (2k+1)\pi/2, \qquad k = 0, 1, 2, 3, \cdots, \tag{55}$$

for which case (52) becomes

$$I_t/I_0 = \tfrac{1}{2}[1 - (-1)^{(k+1)} \sin (\varphi_\perp - \varphi_\parallel)_{ac}]. \tag{56}$$

With this adjustment of φ_c, uniaxial and cubic materials are optically equivalent as far as modulator operation is concerned [compare (53) and (56) with (36) and (37)], so that (39) to (41) for the modulation sensitivity can be applied here as well by changing r_{41} to r_{63}.

The question arises, of course, as to the practicality of compensating for the natural birefringence over a finite aperture; if the modulator is to function properly, the static retardation φ_s must be the same, within a fraction of a radian, for all rays comprising the beam. Three factors are involved here:

(*i*) monochromaticity of the optical source,
(*ii*) dimensional tolerances, and
(*iii*) angular spread in the incident beam.

To illustrate the problem we consider the 0° modulator in KDP. In this configuration the static retardation is given by

$$\varphi_s = 4\pi \frac{\Delta n S}{\lambda_0} \sin \theta_i . \tag{57}$$

If we neglect dispersion in Δn, a range of wavelengths $\Delta\lambda_0$ in the source leads to a spread in φ_s of

$$|\Delta\varphi_s| \approx \varphi_s \left|\frac{\Delta\lambda_0}{\lambda_0}\right| \tag{58}$$

while a variation ΔS in the modulator length results in a spread

$$\Delta\varphi_s \approx \varphi_s \frac{\Delta S}{S} . \tag{59}$$

Under typical circumstances ($\Delta n = 0.04$, $S = 4$ cm, $\theta_i = 19°$, $\lambda_0 = 0.6\ \mu$; see Section VII) φ_s is of order 10^4 radians, so that the requirement $\Delta\varphi_s < 1$ implies that the source monochromaticity and modulator dimensions be maintained within a few parts in 10^5. Although the foregoing tolerances are tight, they are attainable.

A more fundamental problem concerns the angular spread in the incident beam as it traverses the modulating medium. For example, let us suppose that the beam divergence can be characterized by a spread $\Delta\theta_i$ in the angle of incidence. This will produce a variation in φ_s given by

$$\Delta\varphi_s \approx 4\pi \frac{\Delta n S}{\lambda_0} \cos \theta_i \Delta\theta_i \tag{60}$$

so that the inequality $\Delta\varphi_s < 1$ requires that

$$\Delta\theta_i < \frac{\lambda_0}{4\pi\Delta n S \cos\theta_i}. \tag{61}$$

For the example presently under consideration, (61) gives $\Delta\theta_i < 3.2 \times 10^{-5}$ radian = 6.5 sec of arc. Whether or not this requirement can be met depends on the details of the optical system. If, for example, the modulator were operated in the far field of an optical maser of output aperture D which is smaller than the modulator aperture, diffraction alone would produce a spread $\Delta\theta_i \approx 1.22\lambda_0/D$, so that the inequality could be satisfied only if the beam diameter were greater than 2.3 cm, which is clearly unreasonable. On the other hand, if the modulator were placed in the near field of the optical maser, (which extends for a distance D^2/λ_0, which is of order 1 m for a 1-mm diameter beam), diffraction could be negligible, and strain refraction would then set a lower limit to the minimum realizable effective $\Delta\theta_i$, which would in all likelihood still be considerably in excess of the limit set by (61).

In view of the foregoing practical considerations it would seem unreasonable to attempt the construction of an amplitude modulator in the zigzag configuration using a material such as KDP. Moreover, as will be shown in connection with the KDP phase modulator, this material typically requires at least an order of magnitude more power than other materials under consideration.

4.4 *Summary of Results*

The results for the various forms of amplitude modulator may be summarized in a single equation, of the same form as that obtained for the phase modulators

$$\left|\frac{M}{\sqrt{P}}\right| = \frac{2\pi n_0^3}{\lambda_0} ASp\left(\frac{n_0}{\sqrt{\kappa'}}\right) f\left(\frac{\alpha_m S}{2}\right) \sqrt{\frac{2\eta}{\sqrt{\kappa'} hw}}. \tag{62}$$

Values of A and $p(n_0/\sqrt{\kappa'})$ are given in Table II.

V. FACTORS AFFECTING PRACTICAL MODULATOR PERFORMANCE

It is appropriate before discussing the actual design and performance of zigzag modulators to consider some of the practical factors which affect the operation of the device. In particular we consider the effects of

(*i*) fringing fields
(*ii*) deviations from the correct angle of incidence
(*iii*) diffraction

TABLE II — FUNCTIONS APPEARING IN (62) FOR VARIOUS AMPLITUDE MODULATOR CONFIGURATIONS

Modulator	A	$g(\theta_i)$	$p(n_0/\sqrt{\kappa'})$
Linear, 0°	$\frac{1}{2}r_{ij}$	$\frac{1+\cos^2\theta_i}{\sin\theta_i}$	$\frac{2-n_0^2/\kappa'}{n_0/\sqrt{\kappa'}}$
Linear, 90°	$\frac{1}{2}r_{ij}$	$\frac{\cos 2\theta_i}{\sin\theta_i}$	$\frac{1-2n_0^2/\kappa'}{n_0/\sqrt{\kappa'}}$
Quadratic, 0°	$(\rho_1-\rho_2)E_0$	$\sin\theta_i$	$n_0/\sqrt{\kappa'}$
Quadratic, 90°	$(\rho_1-\rho_2)E_0$	$1/\sin\theta_i$	$\sqrt{\kappa'}/n_0$

(*iv*) optical losses
(*v*) lack of parallelism in the reflecting surfaces, and
(*vi*) strain.

5.1 *Effect of Fringing Fields*

The calculations made thus far are strictly correct only in the limit of a uniform microwave field across the active cross section of the modulator. Whether this condition is satisfied or not depends upon the ratio of the width of the electro-optic modulating medium, w, to the width, H, of the parallel plate conductor (see Fig. 6). This ratio, given by

$$\xi = w/H \tag{63}$$

determines the filling factor of the dielectric loaded parallel plate guide. It can be shown from the analysis of Kaminow and Liu[2] that when $\xi = 1$ the field distribution in the modulating medium is uniform and propagates as a TEM wave. This result is, however, valid only when open-circuit boundary conditions prevail at the ends of the waveguide cross section.[2] These boundary conditions will apply physically only to the extent that fringing fields can be neglected. This condition can be expected to be satisfied when the change in transverse impedance in going from the dielectric region to air is large, or alternatively, when the energy stored in the dielectric is large compared to the energy stored in the fringing fields. As long as the dielectric constant of the electro-optic medium is in excess of 10, fringing fields should be negligible and therefore have relatively little effect on the foregoing calculations.

It is important to note that it is generally difficult to propagate TEM or TEM-like waves over a broad band of frequencies in partially loaded

two-conductor transmission lines of the form shown in Fig. 6. This is because dielectric waveguide modes can be supported in such structures at high frequencies. The relative importance of the dielectric modes depends on the filling factor ξ. For filling factors less than unity, three propagating regions can be distinguished.[2] The first occurs at low frequencies where

$$\lambda_m \gg \sqrt{\kappa'} w. \tag{64}$$

In this region the field distribution in the dielectric region is uniform and TEM-like mode propagation results. If, on the other hand, we have

$$\lambda_m \ll \sqrt{\kappa'} w \tag{65}$$

then, as shown in Ref. 2, the microwave energy resides primarily within the dielectric with a cosinusoidal field distribution, and once again propagates as a TEM-like wave. For those cases where $\lambda_m \approx \sqrt{\kappa'} w$ we find that a symmetrical TE_{10}-like waveguide mode propagates with the dispersion characteristic of such a mode.

What is of primary significance here is that for values of the filling factor between

$$0.5 < \xi \leqq 1$$

the dispersion in the microwave phase velocity is small (from the calculations given in Ref. 2 a 30–40 per cent variation in phase velocity results for $\xi = 0.5$). Moreover, as the filling factor approaches unity, not only does the dispersion vanish but the field distribution also becomes uniform. Based upon these considerations it is evident that a parallel plate guide completely filled with a moderately high dielectric constant elec-

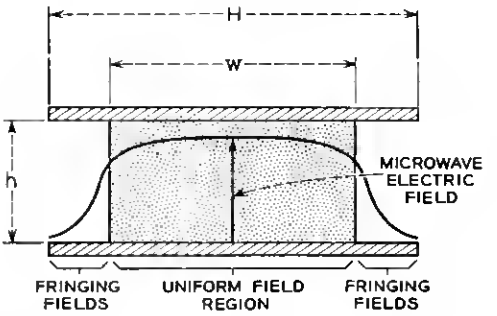

Fig. 6 — Representative microwave electric field distribution in the transverse plane of the modulating medium.

tro-optic material is a suitable practical broadband microwave guiding structure.

5.2 *Sensitivity of the Modulator Performance to Small Changes in the Angle of Incidence*

The velocity matching condition requires that the angle of incidence be adjusted so that $\sin \theta_i = n_0/\sqrt{\kappa'}$. To determine the effect of small deviations from this value, we return to the general expressions for the basic phase modulation processes [(9) and following] and observe that in the lossless case ($\alpha_m = 0$) the modulation sensitivity is always of the form

$$\left| \frac{M}{\sqrt{P}} \right| = C_1 g(\theta_i) \frac{\sin \frac{\beta S}{2}}{\frac{\beta S}{2}} \tag{66}$$

where $g(\theta_i)$ is a slowly varying function of θ_i, and the parameter β is given by [see (8) and (10)]

$$\beta = \beta_m \left(\frac{n_0/\sqrt{\kappa'}}{\sin \theta_i} - 1 \right).$$

Neglecting any variation of $g(\theta_i)$, we find that a variation in θ_i of

$$| \Delta\theta_i | \approx 0.6 \frac{\lambda_m}{S} \frac{n_0}{\kappa'} \left(1 - \frac{n_0^2}{\kappa'} \right)^{-\frac{1}{2}} \tag{67}$$

from the value for perfect velocity matching will reduce the modulation sensitivity by a factor of 2.

5.3 *Diffraction Effects*

Diffraction can limit the performance of the zigzag modulator by producing a divergence in the beam as it passes through the modulator. This is equivalent to a spread in tbe angle of incidence which, for satisfactory modulator operation, must be less than the value of $\Delta\theta_i$ given by (67). Whether or not this requirement can be met depends primarily on whether the modulator is operating in the far or near field of the optical source. The near field of an aperture of diameter D_b illuminated by a coherent plane wave extends a distance of order D_b^2/λ_0. In this region, which is about 1 m for a 1-mm diameter beam, there is little spread. At distances appreciably greater than this, the beam propagates according

to the simple theory of Fraunhofer diffraction, with the main lobe having an angular width[11]

$$\delta\theta \approx \frac{1.22\lambda_0}{D_b}. \tag{68}$$

Thus, in the worst possible case diffraction could result in an effective spread in the angle of incidence of order $1.22\lambda_0/D_b$, and hence limit the allowable value of the ratio of modulator length to beamwidth, according to (67), to

$$\frac{S}{D_d} \leqq \frac{1}{2}\frac{\lambda_m}{\lambda_0}\frac{n_0}{\kappa'}\left(1 - \frac{n_0^2}{\kappa'}\right)^{-\frac{1}{2}}. \tag{69}$$

The aperture D_b is further restricted, in terms of the geometry of the modulator, by the requirement that the beam remain in the modulating medium after the first bounce. From Fig. 1 it is evident that this requires that

$$D_b \leqq 2d \sin \theta_i, \tag{70}$$

where $d = h$ in the 0° modulator, and $d = w$ in the 90° modulator.

Equations (69) and (70) together require that

$$\frac{S}{d} \leqq \frac{\lambda_m}{\lambda_0}\frac{n_0^2}{\kappa'^{\frac{1}{2}}}\frac{1}{(1 - n_0^2/\kappa')^{\frac{1}{2}}}. \tag{71}$$

5.4 *Effect of Optical Losses*

We shall distinguish between two kinds of optical loss. The first arises from scattering due to crystalline inhomogeneities and absorption within the bulk material, and is described by an absorption coefficient α_s. The second is the reflection loss at the mirrors, which are assumed to have a reflectivity R. The optical transmissivity can then be written as

$$I/I_0 = \exp\left[-\alpha_s S \csc \theta_i + (S/d) \cot \theta_i \ln R\right] \tag{72}$$

when $(S/d) \cot \theta_i$, the number of bounces, is large. The relative importance of reflection and absorption losses can be deduced by looking at the ratio, χ, of the quantities in the exponent in (72), i.e.

$$\chi = \frac{1}{\alpha_s d}\cos \theta_i \,|\ln R|. \tag{73}$$

For $\chi > 1$ reflection losses dominate, whereas for $\chi < 1$ the absorption losses are relatively more important.

If we require a certain minimum transmissivity, (72) and (73) fix an

upper limit to the linear dimensions of the modulator in terms of a loss parameter. Thus if $\chi > 1$ and we set $R^{(S/d)\cot\theta_i} = \frac{1}{2}$ in (72), corresponding to a reflection loss of 50 per cent, we obtain

$$\frac{S}{d} \leqq \frac{1}{1 - R} \frac{n_0/\sqrt{\kappa'}}{(1 - n_0^2/\kappa')^{\frac{1}{2}}} \ln 2 \tag{74}$$

when $1 - R \ll 1$. By comparing (71) and (74) we can establish the relative importance of diffraction effects and reflection losses in determining the maximum allowed value of the ratio S/d.* We find that the reflection losses are the important factor whenever the reflectivity is small enough that

$$1 - R > 0.17 \frac{\lambda_0}{\lambda_m} \frac{\kappa'}{n_0} \tag{75}$$

and diffraction effects dominate when the inequality is reversed. For $\lambda_0 = 1\ \mu$, $\lambda_m = 3$ cm (X-band), the quantity $0.17\ \lambda_0/\lambda_m$ is of order 5×10^{-6}. Since even with the best of dielectric multilayers[12] it is difficult to exceed $R = 0.999$ $(1 - R = 10^{-3})$, it is evident that reflection losses are the important factor in materials for which $\kappa'/n_0 \leqq 100$, as is normally the case. An important exception is a ferroelectric operated not far above its Curie point, for which the ratio κ'/n_0 can be very large.

If we now have the situation where $\chi < 1$ and we set $\exp(-\alpha_s S \csc\theta_i) = \frac{1}{2}$ in (72), corresponding to an absorption loss of 50 per cent, we obtain

$$S < \frac{1}{\alpha_s} \frac{n_0}{\sqrt{\kappa'}} \ln 2 \tag{76}$$

with no restriction on d. This equation then sets an upper limit on the modulator length when reflection losses are negligible. For materials having good optical quality where α_s is typically of the order of $0.05\ \text{cm}^{-1}$† such a case might correspond to having $R = 0.999$ and $d \approx 0.2$ mm.

5.5 *Effect of Lack of Parallelism in the Reflecting Surfaces*

A lack of parallelism in the mirrors causes the light and modulating waves to progressively slip out of synchronism, and so degrades the modulator performance. The effect may be estimated as follows.

* By comparing (71) with (74) we are in effect determining the minimum allowed value of the ratio S/d for a fixed sideband amplitude. Such a comparison is of significance since the sidebands carry the modulation information and since their amplitude will determine the signal-to-noise ratio at the detector.

† Accurate values of the absorption coefficients of highly transparent materials are not readily available and are liable to depend on the details of individual sample preparation. A value $\alpha_s = 0.05\ \text{cm}^{-1}$ is a conservative estimate (cf. Ref. 13).

The time T taken for the optical signal to travel the length of the modulator is given by

$$T = \int_0^S \frac{dy}{v_y(y)} \tag{77}$$

where $v_y = (c/n_0) \sin \theta(y)$ is the y component of the optical phase velocity vector (Fig. 7). If the two reflecting surfaces are inclined at an angle ψ, the angle of incidence changes by ψ with each successive bounce. When the total number of bounces N is large, we may approximate $\theta(y)$ by the continuous function $\theta(y) = \theta_i + (N\psi/S)y$, so that the total optical transit time is given by

$$\begin{aligned} T &= \frac{n_0}{c} \int_0^S \sin\left(\theta_i + \frac{N\psi}{S}\, y\right) dy \\ &\approx \frac{n_0}{c} S \sin \theta_i + \frac{n_0}{c} \frac{N\psi S}{2} \cos \theta_i, \qquad \text{for} \qquad N\psi \ll 1. \end{aligned} \tag{78}$$

If the optical and microwave phase velocities are matched at the modulator input ($\sin \theta_i = n_0/\sqrt{\kappa'}$), the first term entering in (78) is just the microwave transit time. Thus at the output of the modulator the optical and microwave signals have shifted, in terms of the microwave phase, by an amount

$$\Delta\varphi = \omega_m \Delta T = \frac{n_0 \omega_m}{c} \frac{S^2}{2d} \frac{\cos^2 \theta_i}{\sin \theta_i} \psi.$$

With the synchronism condition $\sin \theta_i = n_0/\sqrt{\kappa'}$, this becomes

$$\Delta\varphi = \frac{\pi \sqrt{\kappa'} S^2}{d\lambda_m} (1 - n_0^2/\kappa')\psi, \tag{79}$$

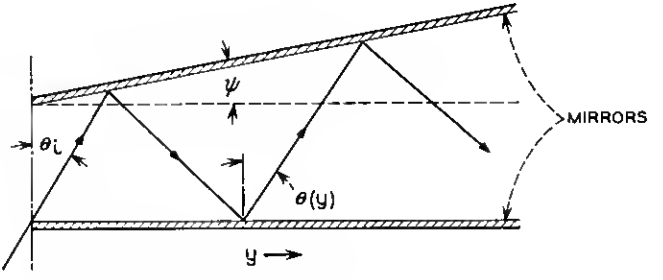

Fig. 7 — Model used in calculating the effect of nonparallelism of the reflecting surfaces.

where λ_m is the free-space modulating wavelength. This phase shift must be less than π if we are to avoid stripping modulation off the beam, since the effect of the modulating field will reverse as the phase shift exceeds π. This leads to a condition on the parallelism of the mirrors

$$\psi < \frac{d\lambda_m}{\sqrt{\kappa'}S^2} \frac{1}{(1 - n_0^2/\kappa')}. \tag{80}$$

5.6 *Effect of Strains*

A complete evaluation of the effect of strain on the modulator performance is very difficult; hence we shall not attempt a complete treatment here. Nonetheless, since strains can have a profound effect on the operation of the modulator, even an approximate treatment such as presented herein can be of value.

In the present discussion it is convenient to consider two broad classes of strain, uniform strain and random strain. The effect of a strain uniform throughout the crystal can be described in terms of a photoelastic matrix[14] which must then be combined with the electro-optic matrix in order to completely describe the optical properties of the crystal. The net effect is to add a static birefringence to that induced electrically.[14] This prohlem can in principle be solved analytically, although a large strain produces an additional complication since it will in general lower the crystal symmetry and hence change the form of the electro-optic tensor. Although cases of quasiuniform strain sometimes occur,* we shall consider here only the case of random strain, since this imposes a more fundamental limitation on device performance.

In a randomly strained crystal where the strain-induced variations occur over distances large compared with an optical wavelength, a ray in progressing through the crystal will see a continuously varying index ellipsoid. If there is little correlation between the shape and orientation of the index ellipsoid at two adjacent points, then a statistical model may be used to study the effect of the strains. Such a calculation is now being carried out and will be reported separately. We confine ourselves here to some general remarks, and a simplified analysis which is valid in the limit of very severe strain.

The general effect of random strain is to partially destroy the spatial coherence of a plane wave traversing the medium, without affecting its

* For example, cubic crystals drawn from a melt are sometimes observed to be uniaxial, with the growth axis as the optic axis.

temporal coherence.* The wave phase at the output of the modulator may then be written as the sum of a coherent and incoherent term, i.e.

$$\Phi(\mathbf{r},t) = \varphi(t) + \delta(\mathbf{r}),$$

where $\delta(\mathbf{r})$ is a random variable, and $\mathbf{r}$ is some suitably defined transverse position vector. Random strains will also mix the two normal modes of the unstrained crystal. We shall not consider the details of this mixing here, but simply assume that there exist at the output of the modulator two orthogonally polarized modes whose wave phases are given by

$$\Phi_{\perp}(\mathbf{r},t) = \varphi_{\perp}(t) + \delta_{\perp}(\mathbf{r}) \tag{81}$$

and

$$\Phi_{\parallel}(\mathbf{r},t) = \varphi_{\parallel}(t) + \delta_{\parallel}(\mathbf{r}) \tag{82}$$

where $\varphi_{\perp}$ and $\varphi_{\parallel}$ are the wave phases in the unstrained crystal as previously calculated, and $\delta_{\perp}(\mathbf{r})$ and $\delta_{\parallel}(\mathbf{r})$ vary more or less randomly across the surface of the beam. In this model the effect of strain on the modulator performance depends on the autocorrelation functions of $\delta_{\perp}$ and $\delta_{\parallel}$, and the cross-correlation between $\delta_{\perp}$ and $\delta_{\parallel}$, as the subsequent analysis will make clear. These correlations will depend on the state of strain of the crystal, and on the length of the optical path, becoming less as the path length increases.

The electric vectors at the output of the modulator can be written in the form

$$e_{\perp}(\mathbf{r},t) = E_{\perp} \exp \{j[\omega t + \varphi_{\perp}(t)] + j\delta_{\perp}(\mathbf{r})\} \tag{83}$$

and

$$e_{\parallel}(\mathbf{r},t) = E_{\parallel} \exp \{j[\omega t + \varphi_{\parallel}(t)] + j\delta_{\parallel}(\mathbf{r})\} \tag{84}$$

where $E_{\perp}$ and $E_{\parallel}$ are the wave amplitudes. From these equations we can show that although strains do not affect the basic phase modulation process, they do affect the over-all modulator-detector system performance. Details depend on the system used, but the following general statement can be made: Any optical communication system in which the modulation or detection process is based upon the heterodyning or homodyning of two optical signals requires that the two signals have relative spatial coherence. Any process that tends to destroy that coherence, such as random strain, will degrade the system performance markedly. It is

* The fact that in general strain will also degrade the collimation of the beam is of importance in some applications. See Appendix B.3.

therefore necessary to be able to evaluate which system will allow us to recover the modulating intelligence with maximum certainty. All modulation-detection schemes presently under consideration fall into three classes

(*i*) amplitude modulators followed by quantum counters,

(*ii*) phase or amplitude modulators followed by optical heterodyne or homodyne detectors, and

(*iii*) phase modulators followed by optical frequency discriminators and then by quantum counters.

Starting with (83) and (84), we analyze these three classes in Appendix B. The results are summarized below.

5.6.1 *Amplitude Modulators followed by Quantum Counters*

As discussed in Section IV, the amplitude modulator consists of a system in which two phase-modulated waves of the form given by (83) and (84) are combined in an analyzer. As shown in Appendix B, the time-varying intensity transmitted by the analyzer is proportional to an integral of the form [see (118)]

$$\int_s \begin{matrix} \sin \\ \cos \end{matrix} \left\{ \delta_\perp(\mathbf{r}) - \delta_\parallel(\mathbf{r}) \right\} da \tag{85}$$

the integration being taken over the cross section of the beam. In the case of severe random strain, when $\delta_\perp$ and $\delta_\parallel$ can *independently* take on all values (i.e., no cross-correlation between $\delta_\perp$ and $\delta_\parallel$), the integral (85) vanishes and there is no amplitude modulation. More moderate strain would result in a nonzero depth of modulation which would, however, be less than that attainable in a strain-free crystal.

5.6.2 *Heterodyne or Homodyne Operation*

In heterodyne or homodyne operation the modulated signal is mixed with a second locally generated optical signal to obtain a microwave intermediate frequency which is then detected conventionally. Assuming a square-law detector and a strong local oscillator having both spatial and temporal coherence, the output signal at the difference frequency is proportional to [Appendix B, (121)]

$$\int_s \begin{matrix} \cos \\ \sin \end{matrix} \left\{ \delta_{\perp,\parallel}(\mathbf{r}) \right\} da \tag{86}$$

which vanishes in the limit of very bad strain where $\delta_\perp$ and $\delta_\parallel$ can take on all values.

Thus in this mode of operation, too, strains result in a reduced detector output. The effect here is likely to be more severe than in the case of the simple amplitude modulator-quantum counter system, since for a given degree of strain the autocorrelation of $\delta_\perp$ or $\delta_\parallel$ is expected to be less than the cross-correlation of $\delta_\perp$ and $\delta_\parallel$. Thus, in a given crystal the integral (85) is liable to have a larger value than the integral (86).

5.6.3 *Phase Modulators Followed by Frequency Discriminators*

In the third system under consideration phase modulation is directly converted to amplitude modulation in some frequency-selective optical circuit[15,16] of which a Fabry-Perot etalon is perhaps the simplest example. Spatial coherence per se plays no essential role here. Analytically, as is shown in Appendix B, the integral analogous to the ones given by (85) and (86) which arises in this case has the form [see 124]

$$\int_S |\exp\left[j\delta_{\perp,\parallel}(\mathbf{r})\right]|^2 \, da. \tag{87}$$

This of course has a constant value equal to the beam area and can therefore not influence the system response. However, strain can still adversely effect this system to the extent that the discriminator performance is degraded by loss of collimation in the transmitted beam.

Thus strain will *always* be a problem in optical modulators. In fact the preceding considerations show that the presence of severe random strain will result in no useful output from those modulation-detection schemes which rely on the *interference* of two beams. In this case only the phase modulator-frequency discriminator system has any real chance of success.

VI. OPTIMUM DESIGN PROCEDURE

6.1 *Choice of Modulator Dimensions*

For the purpose of discussing the optimization of modulator dimensions as well as the choice of operating temperature, a useful figure of merit is the product of the modulation sensitivity and the optical transmissivity, which for *all* modulators can be written as

$$\mathfrak{F} \equiv \left|\frac{M}{\sqrt{P}}\right| \frac{I}{I_0} = \frac{2\pi}{\lambda_0} n_0^3 S \sqrt{\frac{2\eta}{\sqrt{\kappa'} dl}} \begin{Bmatrix} \frac{1}{2} r_{41} \\ \text{or} \\ \rho E_0 \end{Bmatrix} p\left(\frac{n_0}{\sqrt{\kappa'}}\right) f\left(\frac{\alpha_m S}{2}\right) \times \exp\left[-\frac{\sqrt{\kappa'}}{n_0} S\left(\alpha_S - \frac{1}{d} \ln R \sqrt{1 - \frac{n_0^2}{\kappa'}}\right)\right]. \tag{88}$$

Here d is the distance between the reflecting surfaces (either h or w, depending on whether the 0° mode or the 90° mode is used), and l is the width of the reflecting surfaces; recall that S is the modulator length. The remaining functions $f(\alpha_m S/2)$ and $p(n_0/\sqrt{\kappa'})$ have been defined above in (12) and Tables I and II respectively. Equation (88) applies when we have velocity matching.

The optimum modulator dimensions can now be found by maximizing the figure of merit. It is evident that the dimension l should be made as small as possible. If the beam diameter D_b is specified, this then determines the minimum value of l, $l_{\min} = D_b$. The mirror spacing d may next be chosen so as to maximize (88), the appropriate value being

$$d_{\text{opt}} = -2S \ln R \frac{\sqrt{\kappa'}}{n_0} \left(1 - \frac{n_0^2}{\kappa'}\right)^{\frac{1}{2}}. \tag{89}$$

The ratio S/d obtained from this equation corresponds to a reflection loss of roughly 50 per cent. It is worth pointing out that for practically attainable reflectivities, this optimum value of S/d is less than the maximum value set by diffraction effects [see (77)], and so represents a reasonable design value.

When the optimum value of d given by (89) is substituted back into (88), there results an equation for $\mathfrak{F}$ which depends only on S; S may then be chosen so as to maximize this figure of merit. The optimum value, S_{opt}, is defined by the transcendental equation

$$\frac{1}{\exp \alpha_m S_{\text{opt}} - 1} - \frac{1}{2\alpha_m S_{\text{opt}}} = \frac{\sqrt{\kappa'}}{n_0} \frac{\alpha_s}{\alpha_m}. \tag{90}$$

In the absence of optical absorption ($\alpha_s = 0$), the optimum length is given by $\alpha_m S_{\text{opt}} = 1.25$. As α_s increases, the optimum length decreases, as shown in Fig. 8. When the inequality $(n_0/\sqrt{\kappa'})(\alpha_m/\alpha_s) \ll 1$ is satisfied, we find that the optimum length is determined solely by the optical attenuation, and is given by

$$S_{\text{opt}} = \frac{n_0}{2\sqrt{\kappa'}\alpha_s}. \tag{91}$$

The dimensions of the modulator are thus completely determined: l by the beamwidth, d by the optical reflection losses and S by the microwave and optical attenuation constants. For materials having sufficiently low microwave and optical losses, the optimum length given by (90) may be greater than any practically realizable crystal length. Under these circumstances one should make S as large as possible, and then choose d to satisfy (89).

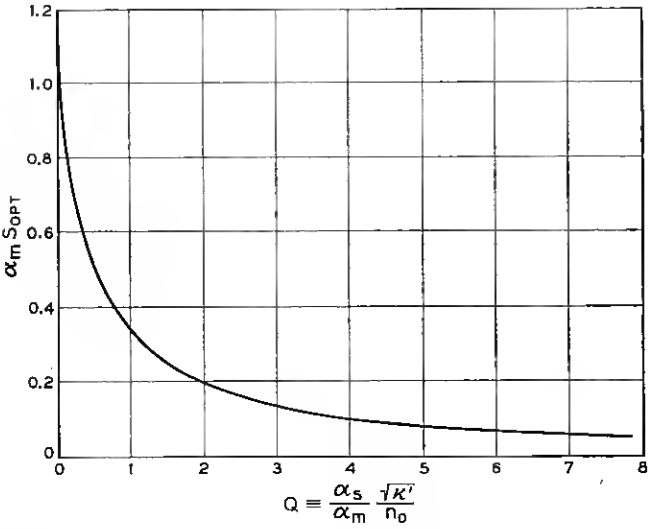

Fig. 8 — Dependence of optimum modulator length on optical and microwave loss parameters.

6.2 *Choice of Operating Temperature*

The dielectric and electro-optic constants of useful modulating materials are strongly temperature-dependent. In ferroelectrics, for example, both the electro-optic coefficients and the microwave losses increase dramatically near the Curie point. We should thus like to establish whether there exists a preferred operating temperature which maximizes the figure of merit [see (88)] independently of the modulator dimensions.

We begin by assuming that the modulator dimensions bave been optimally chosen according to the results of the preceding section. With this choice of dimensions, (88) becomes

$$\mathfrak{F}_{opt} = \frac{2\pi}{\lambda_0} n_0^3 \sqrt{-\frac{\eta}{\sqrt{\kappa'} D_b \ln R}} \begin{Bmatrix} \frac{1}{2} r_{41} \\ \text{or} \\ \rho E_0 \end{Bmatrix} p\left(\frac{n_0}{\sqrt{\kappa'}}\right) \left[\frac{n_0/\sqrt{\kappa'}}{\alpha_m(1 - n_0^2/\kappa')^{\frac{1}{2}}}\right]^{\frac{1}{2}} \times e^{-\frac{1}{2}} \left[\sqrt{u} e^{-Qu} f\left(\frac{u}{2}\right)\right] \quad (92)$$

where $u = \alpha_m S_{opt}$ is found from (90) and where we introduce the notation $(\alpha_s/\alpha_m)(\sqrt{\kappa'}/n_0) \equiv Q$. The function $g(u) = \sqrt{u} e^{-Qu} f(u/2)$ is, through (90), an implicit function of the independent variable Q. The function may be approximated as

$$g(Q) \approx 0.214 \frac{\left[1 - \exp\left(-\frac{3}{2}\sqrt{Q}\right)\right]}{\sqrt{Q}}.$$

For a TEM-like wave, the microwave attenuation constant is given in terms of the dielectric constant and loss tangent of the medium by

$$\alpha_m = \frac{\pi}{\lambda_m}\sqrt{\kappa'}\tan\delta. \tag{93}$$

The figure of merit can now be approximated solely in terms of material parameters as

$$\mathfrak{F}_{\text{opt}} = 15.8\frac{n_0^4}{\lambda_0}\frac{1}{\sqrt{-\alpha_S D_b \ln R}}\frac{1}{\kappa'^{\frac{1}{2}}}\left\{\begin{matrix}\frac{1}{2}r_{41}\\ \text{or}\\ \rho E_0\end{matrix}\right\}p\left(\frac{n_0}{\sqrt{\kappa'}}\right) \times\left\{\frac{1 - \exp\left[-\frac{3}{2}\left(\frac{\alpha_S\lambda_m}{\pi n_0\tan\delta}\right)^{\frac{1}{2}}\right]}{(1 - n_0^2/\kappa')^{\frac{1}{2}}}\right\} \tag{94}$$

where all the numerical constants, including the impedance of free space, $\eta = 377$ ohms, have been combined into a single factor.

Once the temperature dependence of the electro-optic coefficient, dielectric constant and loss tangent are known,* (94) can be used, at least in principle, to select an optimum operating temperature.

Further analytical progress requires some assumption of the temperature dependence of these coefficients as well as a choice of the mode of operation. To be definite we select the mode for which $p(n_0/\sqrt{\kappa'}) = \sqrt{\kappa'}/n_0$. As may be seen from Tables I and II, this is the most favorable value that can be realized and applies, for example, to the linear, 0° phase modulator.

The temperature coefficient of the linear electro-optic coefficient is expected to follow that of the dielectric constant.[17] The reason for this is as follows: The electro-optically induced birefringence arises fundamentally from a change in the polarization, rather than the applied field, and in fact Pockel's[18] original formulation of the electro-optic effect was in terms of constants e_{ij} relating the coefficients of the index ellipsoid to the induced polarization. The r_{ij} coefficients used here are related to Pockel's e_{ij} by

$$r_{ij} = \epsilon_0(\kappa' - 1)e_{ij}.$$

* The index of refraction, n_0, to the extent to which it is determined by the electronic polarizability, should be almost independent of temperature.

Thus for materials having a high dielectric constant we expect r_{ij} to be approximately proportional to κ', and to the extent that the coefficients e_{ij} are temperature independent,[17] to have the same temperature dependence as κ'.

A similar argument in the case of the quadratic effect leads to the conclusion that ρ should be proportional to κ'^2. Here, however, the situation is complicated by the fact that the bias field E_0, which for optimum operation should be as large as the breakdown field strength of the material permits, will be temperature-dependent whenever this breakdown field strength is temperature-dependent. In many solids we expect dielectric breakdown to occur at some definite value of internal field. In materials of high dielectric constant the internal field is determined by the polarization, so that the breakdown field strength, and hence the allowed dc bias, will be inversely proportional to κ'. The net result is that the product of ρE_0 may be taken proportional to the first power of κ', and the quadratic and linear effects become formally identical.

The preceding assumptions allow us to write the figure of merit for a given material wholly in terms of its dc and optical dielectric parameters, so that $\mathfrak{F}$ becomes proportional to

$$\frac{\kappa'^{\frac{3}{2}}}{(1 - n_0^2/\kappa')^{\frac{1}{4}}}\left[1 - \exp\left(-\frac{3\lambda_m \alpha_S}{2\pi n_0 \tan \delta}\right)^{\frac{1}{2}}\right]. \tag{95}$$

We must now distinguish between low and high microwave losses, the criterion being the magnitude of the ratio $3\lambda_m\alpha_S/2\pi n_0 \tan \delta$. For sufficiently low microwave losses, the exponential factor in (95) will disappear, so that the figure of merit is proportional simply to $\kappa'^{3/2}/(1 - n_0^2/\kappa')^{1/4}$. Since the ratio n_0^2/κ' will always be substantially less than unity, the optimum operating temperature is that which maximizes κ'. For ferroelectric materials this will mean lowering the temperature to the vicinity of the Curie point, T_c. Of course the losses will normally increase as the temperature is lowered, so that at some point the approximation of low microwave loss breaks down. For sufficiently high loss we may expand the exponential term in (95), obtaining a figure of merit proportional to

$$\frac{1}{(1 - n_0^2/\kappa')^{\frac{1}{4}}}\sqrt{\frac{\kappa'^{\frac{1}{2}}}{\tan \delta}}. \tag{96}$$

For ferroelectrics such as KDP[19,20] or $SrTiO_3$[21,22] in which both κ' and $\tan \delta$ are dominated by a $(T - T_c)^{-1}$ dependence, T_c being the Curie temperature, this result says that operation near the Curie point is

favored (although not strongly) even in the presence of substantial microwave loss.

6.3 *Bandwidth Limitations: Design of Optical Coupler*

The question of the bandwidtb of tbe zigzag modulator has two aspects — microwave bandwidth and optical bandwidth. Since both the optical and modulating signals propagate as TEM-like waves, it might at first be thought tbat the bandwidth would be limited only by the dispersion in the material parameters of the modulating medium. For most materials this would imply a microwave bandwidth as large as 10 or 20 gc, and since the fractional optical bandwidth required to accommodate even microwave frequency sidebands is very small (of order 10^{-5}), optical dispersion should never be a problem.

A more discriminating analysis of the question of bandwidth reveals, however, that the physical dimensions of the modulator limit the realizable bandwidth, especially when these dimensions are optimized so as to obtain the ultimate in low-power performance. In an optimum design the length S_{opt} and width (or height) d_{opt} are uniquely determined by the electrical properties of the modulating medium both at microwave and optical frequencies as well as the loss properties of the medium [see (89) through (91) and the attendant discussion]. For highly transparent low-loss microwave materials, d_{opt} computed from (89) is nominally in the order of a few tenths of a millimeter and S_{opt} is usually several centimeters (see Table IV in Section VII for typical results). The one dimension which remains unspecified is the beam diameter D_b. As remarked above in Section 6.1, D_b should be chosen as small as possible and yet remain within the diffraction limits of the device over the length S_{opt}. Accordingly, we find that, based upon certain operational practicalities and diffraction limits, D_b must normally be restricted to about a millimeter. Thus, as the aperture of the device is typically an order of magnitude larger than the spacing between mirrors, it is impossible to satisfy (70); i.e., the beam bounces back out of the modulator, and hence cannot be confined to the active area of the device by means of a simple aperture arrangement. In such cases the beam can be confined to the interior of the modulator only if we include an appropriate optical coupler at the input (and output) of tbe modulator.

It is shown in Appendix C that a suitable coupler which allows all of the incident optical energy to be transferred into the active medium of the modulator is a Fabry-Perot resonator of the form shown either in Fig. 10(a) or Fig. 11. The physical operation of the coupler is easily understood when one observes that because of its finite length energy must

leak off to the right into the interior of the modulator. Then by properly adjusting the spacing between reflectors as well as the reflectance of the lower reflector it is possible to completely cancel the reflected wave, and have the energy trapped in the coupler section walk off into the modulator. Expressions for the required spacing and reflectance are derived in Appendix C. Here we simply point out that such a coupler can be realized in a typical case with reflectivities in the neighborhood of 99 per cent, which is easily attained, and with dimensions L_c and l_c of the same order as D_b and d_{opt}, respectively.

We are now in a position to examine the bandwidth limitations imposed by the coupler and modulator dimensions. The bandwidth is generally determined by three factors. In order of importance these are

(*i*) the spacing l_c and loaded Q of the coupler,

(*ii*) the size of D_b compared with the microwave modulating wavelength, and

(*iii*) the microwave impedance of the structure.

The last factor, microwave impedance, is of practical significance because the impedance of the modulator will inevitably be low, and it becomes progressively more difficult to obtain a broadband match into a transmission line as its impedance is lowered. However, a number of standard microwave techniques are available to overcome this difficulty.

The second factor, the beam diameter, affects the bandwidth in the following way. In order that the microwave modulation be detectable in a direct simple way it is necessary that the modulation frequency phase be approximately constant across a given section of the beam. Hence it is necessary that the projection of the beam cross section along the axis of the structure be appreciably less than half the microwave wavelength in the medium. Mathematically

$$D_b \ll \frac{\lambda_m}{2 \cos \theta_i \sqrt{\kappa'}} \tag{97}$$

where λ_m is the free-space wavelength.

Finally, with reference to the first factor, the coupler spacing and loaded Q, we note that in order to avoid microwave impedance discontinuities in the low-impedance modulator line it is mandatory that l_c and d be very nearly equal. If the spacing d is then kept small so as to obtain the lowest possible modulating power, the input coupler will limit the bandwidth in the following way. The Fabry-Perot coupler will be resonant at a series of frequencies spaced by

$$\Delta f = \frac{c}{2n_0 l_c \cos \theta_i}. \tag{98}$$

The base bandwidth δf of the coupler will be determined hy the Q of an individual mode, and can be shown from Appendix C to be

$$\delta f = \frac{1}{\pi}\frac{c}{D_b}\frac{\sin\theta_i}{n_0}\begin{cases}\sqrt{1 - n_0^2\sin^2\theta_i} & \text{for } n_0^2 < \sqrt{\kappa'} \\ \cos\theta_i & \text{for } n_0^2 > \sqrt{\kappa'}.\end{cases} \tag{99}$$

Since this bandwidth is available in each of the Fabry-Perot modes, microwave subcarrier operation at frequencies above this baseband is allowed[23] provided that the subcarrier frequency (or optical sideband) is some multiple of the mode spacings given by (98). The problem, of course, is that the mode spacings become very large when the coupler reflector spacing l_c is small, and since l_c must be comparable with the modulator thickness d, it follows that the lowest allowed microwave subcarrier will be at much too high a frequency when d is adjusted to its optimum value of a fraction of a millimeter (e.g., $d = 0.2$ mm corresponds to $\Delta f \approx 300$ gc). It is evident then that the minimum power configuration is restricted to baseband operation with a bandwidth determined either by (97) or (99), whichever is smaller. For $D_b = 1$ mm, (97) gives $f_m \lesssim 10$ gc when the modulating medium is a ferroelectric such as strontium titanate, while (99) gives $\delta f \approx 5$ gc.

Greater bandwidth can be obtained, at the expense of increased modulation power, by making the thickness d considerably greater than optimum. If d is made sufficiently large (e.g., 3.6 mm in the case of the strontium titanate modulator), a simple input aperture can be used in place of the Fabry-Perot coupler.* This removes the frequency limitations set by (98) and (99), leaving only that imposed by the finite beam width (97) and material dispersion. The frequency limitation imposed by the beam width is quite fundamental. In fact, when the projection of the beam diameter along the axis of the modulator is exactly equal to a full microwave wavelength in the material there results no net modulation. We therefore define a cutoff frequency for the modulator as

$$f_c = \frac{c}{D_b\cos\theta_i\sqrt{\kappa'}}. \tag{100}$$

In summary, then, we find that in order to fully exploit the low modulation power requirements of the zigzag modulator it is necessary to restrict the frequency of operation for most substances to a few gc at baseband,† and to use a relatively sophisticated coupler to get the optical

* If $n_0^2 > \sqrt{\kappa'}$ it will be necessary to use a more complex aperture analogous to the one shown in Fig. 11.

† For CuCl the operating frequency can be as high as about 20 gc (see Table IV in Section VII).

energy into the device. By relaxing the power requirements the upper frequency limit can be extended above 10 gc in a relatively simple structure. Examples of both kinds of design are given in the following section.

VII. DISCUSSION AND CONCLUSIONS

We have analyzed in detail the behavior of zigzag phase and amplitude light modulators (Sections III and IV) as well as the basic underlying theory for this class of modulators (Section II). Our treatment differs from the work of other investigators[1-3] along these lines in a number of crucial ways. We have included microwave losses in the initial calculation of the optical retardation and have considered the 90° mode of operation in addition to the originally proposed 0° mode for several different classes of electro-optic media. The analysis has been detailed enough and has treated enough of the important practical factors which limit the operation of the device (Section V), so that a realistic optimum design procedure can be presented (Section VI). In essence, this procedure requires that the dimensions of the modulator be so chosen that all of the incident microwave power be confined to as small a volume of the electro-optic material as the microwave, optical, and reflection losses will permit. As a result, large modulating field strengths are obtained with moderate amounts of power.

Based upon our treatment we find that there are three main aspects to broadband modulator design. The first is the velocity synchronism condition; here we find that the basic phase velocity matching criterion is unaffected by microwave loss. The second is the effect of modulator dimensions and aperture on bandwidth. These problems have been discussed in Section 6.3, where it was shown that the aperture limits the highest modulating frequency in a fundamental way [see (100)] and that the other dimensions in effect determine the requisite coupling scheme (either Fabry-Perot or simple aperture) and thence the bandwidth. The final criterion of significance is the strain properties of the modulator crystal (Section 5.6). Crystalline strain is a serious problem in all forms of electro-optic amplitude modulators, but is particularly deleterious in the traveling-wave modulator because of the long optical path.

We are now in a position to present some actual designs of zigzag phase and amplitude light modulators as well as the performance to be expected of these devices. Before doing so, however, we first summarize in Table III the pertinent microwave and optical material parameters, to the extent that they are known, for a number of electro-optic modulating crystals which are currently available. With regard to the data presented in Table III, much of which is tentative, two points should be noted.

TABLE III — MATERIAL PARAMETERS FOR SOME ELECTRO-OPTIC CRYSTALS

Material	T_c	T	$(\rho_1 - \rho_2)$*	r_{61}†	r_{63}†	n_0	κ'	tan δ	Remarks
$BaTiO_3$	393°K	393°K 403°K	23×10^{-12} 6.5×10^{-12}			2.4 2.4	6000 4500	0.5 0.4	Electro-optic data apply at $\lambda_0 = 5021$ A and $f \leqq 200$ kc (Ref. 24). Microwave data apply at 24 gc (Ref. 25).
$SrTiO_3$	33°K	77°K 293°K	0.31×10^{-12} 0.194×10^{-12}			2.409 2.409	1500 300	1.25×10^{-3} 1.5×10^{-3}	Electro-optic data apply at $\lambda_0 = 6328$ A and $f < 1$ kc. Data obtained from Ref. 26. Value for n_0 applies at $\lambda = 5891$ Å. Microwave data apply at 20 gc (Refs. 21, 27, 28).
$KTaO_3$	≈1°K	4°K 77°K	4.3×10^{-12} 0.1×10^{-12}			2.5 2.5	4400 800	0.72×10^{-4} 0.2×10^{-3}	Electro-optic data apply at $\lambda = 6328$ A and $f < 1$ kc (Ref. 29). Microwave data apply for frequencies below 20 gc (Ref. 29).
CuCl		293°K		6×10^{-10}		1.93	8.3	1×10^{-2}	Electro-optic data measured at dc (Ref. 30). Microwave data measured at 5 gc (Ref. 31).
ZnS		293°K		2.4×10^{-10} 1.2×10^{-10}		2.368	10.25	2×10^{-3}	Electro-optic data measured at dc (2.4×10^{-10}) and 3 gc (1.2×10^{-10}). Microwave data measured at 5 gc.
KDP	120°K	173°K 293°K			6.8×10^{-10}	1.468 1.468	60 20.2	17.5×10^{-3} 7.5×10^{-3}	Electro-optic data apply at high frequencies, $f_c > 100$ kc, and for $4000 < \lambda_0 < 7000$ Å (Ref. 32). Microwave data apply at 9.2 gc (Ref. 33).
ADP	148°K	173°K 293°K			5.5×10^{-10}	1.479 1.479	16 14	6.5×10^{-3} 6×10^{-3}	T_c refers to antiferroelectric phase transition (Ref. 34). Electro-optic data apply at high frequencies, $f > 100$ kc, and for $4000 < \lambda_0 < 7000$ Å (Ref. 32). Microwave data apply at 9.2 gc (Ref. 33).

* Expressed in units of cm^2/V^2.
† Expressed in units of cm/V.

The first is that the microwave properties for the different materials listed have not all been measured at the same frequency. For simplicity we shall assume that there is negligible dispersion in the microwave parameters. The same assumption is made for the optical data. The second point to be noted is that the data available for the electro-optic coefficients apply in most cases at very low frequencies. Hence the values for the electro-optic coefficients represent the unclamped values and consequently overestimate in many cases the desired microwave or clamped values for these coefficients. Thus this table should be viewed simply as a guide to the material parameters. From the data given in Table III we select three materials, CuCl, $SrTiO_3$ and KDP, as being the best in their respective crystalline classes. Each of these materials combines good microwave properties (low loss with high intrinsic impedance) with a large electro-optic coefficient. With reference to $SrTiO_3$ it should be noted that the quadratic effect exhibited by this material is anomalously high, as it is with $BaTiO_3$ and $KTaO_3$, the effect being 10^5–10^7 times higher than in the best glasses. When one couples this together with the fact that the "effective linear coefficient" for quadratic materials is ρE_0, one immediately sees from the data listed in Table III that for $E_0 > 1000$ v/cm, quadratic materials are potentially as good as if not better than linear materials.

It is instructive to carry out two designs. One, based on the optimum design procedures of Section 6.1, results in a modulator requiring an absolute minimum of modulating power. However this design requires the use of an input optical coupler and is inherently narrow-band. In another, more practical design, the mirror spacing d is chosen to allow the use of a simple aperture. In this design we obtain increased bandwidth at the expense of higher modulating power. Tables IV and V summarize the design parameters, expected performance, and several of the practical limitations for each of these designs. Note that we do not include an amplitude modulator design for KDP. The reason, of course, is the difficulty encountered in trying to compensate for the static retardation in such a material (See Section 3.3.)

In order to carry out the calculations several design parameters were chosen independently as a matter of convenience. Thus the optical wavelength was taken as the visible red line of the He-Ne gas laser at 6328 Å, and in the absence of experimental data the optical absorption coefficient α_s was assumed to have the same value as that found in good optical glasses, viz., $\alpha_s \approx 0.05$ cm^{-1}. The multilayer reflectivity was taken as 0.999, about as high as is practically achievable.[12] A reflectivity this high is essential if the ultimate in low-power modulation is to be obtained in

the optimum design, but the requirements can be relaxed considerably in the practical design. For example, a decrease in reflectivity to 0.982 increases the optical insertion loss of the practical $SrTiO_3$ modulator by only 1.7 db.

In the absence of any really complete temperature data we have taken room temperature, 300°K, as an operating temperature. Although it is true that for the ferroelectrics, $SrTiO_3$ in particular, the temperature analysis of Section VI shows that the modulating power is reduced somewhat as we approach the Curie point, the concomitant increase in κ' reduces θ_i below the practical minimum and at the same time reduces the available bandwidth by decreasing the microwave wavelength in the material [see (97) and accompanying discussion]. Thus 300°K is in fact close to the practical optimum operating temperature for $SrTiO_3$.

The operating frequencies given in Tables IV and V have been arrived at by the following considerations. A practically realizable aperture which remains within diffraction limits is nominally 1 mm. The *optimum* design therefore requires the use of a coupler with restricted bandwidth. The data of Table IV are thus calculated for a modulating frequency of 5 gc, which is within the passband of all modulators. In Table V the operating frequency has been chosen as 10 gc and is in all cases less than the cutoff frequency. What should be noted here is that by ignoring the bandwidth problem, we obtain in the optimum design shown in Table IV the irreducible minimum microwave modulating power. In the case of the practical design listed in Table V the spacing between mirrors d has been increased to allow the use of a simple aperture. The price we pay, of course, is in increased modulating power. We should also make special note of the fact that from a practical viewpoint the impedance level of the design given in Table V is much more favorable than for the one given in Table IV. The restriction on the maximum attainable modulating frequency in the practical design is the aperture size [see (97)].

The column headed "configuration" in Tables IV and V deserves some comment. For each material considered, the configuration chosen was the one for which the function $p(n_0/\sqrt{\kappa'})$ had its maximum value. In the case of $SrTiO_3$ there are three possible configurations for the phase modulator. Table I shows that the 0° phase modulator (PM) in the $\perp$-mode and the 90° PM in either the $\perp$ or $\parallel$-modes are all equally suitable choices. We should bear in mind at this point that for $SrTiO_3$ (as well as $BaTiO_3$ and $KTaO_3$), it is only the difference in the electro-optic coefficients $|\rho_1 - \rho_2|$ that is known (see Table III) and not ρ_1 or ρ_2 alone. However, since in an amorphous material ρ_2 is identically zero (Appendix A) we expect that in a cubic material $|\rho_2|$ will still be

TABLE IV — OPTIMUM MODULATOR PERFORMANCE FOR SEVERAL ELECTRO-OPTIC MATERIALS. MODULATING FREQUENCY, 5 GC; OPTICAL WAVELENGTH, 6328 Å; TEMPERATURE, 300°K

Material	Configuration	θ_i	$\lvert\Delta\theta_i\rvert$	ψ_{max}	D_b	d_{opt}	S_{opt}	δf	IL^*	$P(M = \frac{1}{2})$	Remarks
CuCl	0°-PM; ⊥-mode	42.1°	9.5°	0.072°	1 mm	0.15 mm	6.7 cm	24.7 gc	4.3 db	0.315 w	S_{opt} fixed by optical losses. Dimensions are within limits set by diffraction.
	0°-AM	42.1°	9.5°	0.072°	1 mm	0.15 mm	6.7 cm	24.7 gc	4.3 db	0.13 w	
$SrTiO_3$	0°-PM; ⊥-mode	8°	1.18°	0.2°	1 mm	0.20 mm	1.4 cm	5.2 gc	4.3 db	0.17 w	S_{opt} fixed by optical losses. Dimensions are within limits set by diffraction. Results apply for E_0 = 30 kv/cm. Computations for phase modulator treat material as amorphous.
	90°-AM†	8°	1.18°	0.2°	1 mm	0.20 mm	1.4 cm	5.2 gc	4.3 db	0.17 w	
KDP	0°-PM; ⊥-mode	19.1°	4.84°	0.15°	1 mm	0.19 mm	3.3 cm	18.7 gc	4.3 db	2.8 w	S_{opt} fixed by optical losses. Dimensions are within limits set by diffraction.

* The insertion loss does not take reflection losses into account. These can be eliminated in any one of a number of standard ways.
† In the case of the amplitude modulator, a bias field of 30 kv/cm results in operating at a mode number of $m \approx 600$.

TABLE V — PRACTICAL MODULATOR PERFORMANCE FOR SEVERAL ELECTRO-OPTIC MATERIALS. MODULATING FREQUENCY, 10 GC; OPTICAL WAVELENGTH, 6328 Å; TEMPERATURE, 300°K

Material	Configuration	θ_i	$\lvert\Delta\theta_i\rvert$	ψ_{max}	D_b	d	S	f_c	IL^*	$P(M = \frac{1}{4})$	Remarks
CuCl	0°-PM; ⊥-mode	42.1°	4.8°	0.18°	1 mm	0.75 mm	6.7 cm	140 gc	2.6 db	1.6 w	S fixed by optical losses. Dimensions are within limits set by diffraction.
	0°-AM	42.1°	4.8°	0.18°	1 mm	0.75 mm	6.7 cm	140 gc	2.6 db	0.66 w	
$SrTiO_3$	0°-PM; ⊥-mode	8°	0.59°	1.8°	1 mm	3.6 mm	1.4 cm	17.5 gc	2.6 db	3.1 w	S fixed by optical losses. Dimensions are within limits set by diffraction. Results apply for $E_0 = 30$ kv/cm. Computations for phase modulator treat material as amorphous.
	90°-AM†	8°	0.59°	1.8°	1 mm	3.6 mm	1.4 cm	17.5 gc	2.6 db	3.1 w	
KDP	0°-PM; ⊥-mode	19.1°	2.42°	0.61°	1 mm	1.53 mm	3.3 cm	70.7 gc	2.6 db	23 w	S fixed by optical losses. Dimensions are within limits set by diffraction.

* The insertion loss does not take reflection losses into account. These can be eliminated in any one of a number of standard ways.
† In the case of the amplitude modulator a bias field of 30 kv/cm results in operating at a mode number $m \approx 600$.

substantially less than $|\rho_1|$, so that we may take the measured value of $|\rho_1 - \rho_2|$ as an approximate measure of $|\rho_1|$ alone. This has been done wherever necessary.

The remaining parameters listed in Tables IV and V require little or no further comment. The angle of incidence θ_i necessary to achieve velocity synchronism is given together with the deviation in θ_i, $|\Delta\theta_i|$, which results in a 3-db degradation in modulation sensitivity. The angle ψ_{max} is the maximum permissible angular deviation in the parallelicity of the mirrors if the performance is to be degraded by less than 3 db. The modulator dimensions are contained in D_b, d_{opt} or d, and S_{opt} or S depending upon which design is being considered. The column headed IL in the tables refers to the optical insertion loss suffered in traversing the modulator. Finally, the quantity $P(M = \frac{1}{2})$ is the microwave modulating power required to achieve a modulation index of 0.5.

It is worth mentioning at this point that Tables IV and V implicitly contain several idealizations. The first is that the crystals are strain-free. For KDP this assumption is approximately justified, but for CuCl and $SrTiO_3$ it is far from reality and, as noted previously, could seriously degrade the performance of the amplitude modulator. The second idealization comes from the assumption that the modulating field is uniform over the entire cross section of the crystal. In any practical modulator this will not be strictly true. However, to the extent that fringing fields can be neglected in a parallel plate line completely filled with electro-optic material, this assumption is realizable (see Section 5.1). In consequence, the calculations made for the required modulating power should be reasonably accurate. The primary factor which would cause an increase in modulating power is a deviation from the correct angle of incidence. However, the tolerances in θ_i given in Tables IV and V are sufficiently large that maintaining the required angle should present no problem. Finally we should point out that we have assumed that a dc bias as large as 30 kv/cm can be applied to the $SrTiO_3$ sample without dielectric or interfacial breakdown, and that the electro-optic effect does not saturate at these high fields. It is clear that a high dc bias field is desirable with the $SrTiO_3$ modulator, since this increases the effective linear electro-optic coefficient ρE_0.

The results given in Tables IV and V demonstrate that broadband microwave modulation of light can be effected with very little modulating power. In a practically realizable design, we find that a 1 mm × 3.6 mm × 1.4 cm rectangular slab of $SrTiO_3$ biased with 30 kv/cm should produce 50 per cent linear modulation of light with less than 5 watts of power at any modulating frequency from dc to 10 gc. A CuCl slab of

dimensions 1 mm × 0.75 mm × 6.7 cm should require still less power (≈1–2 w) without the need of any dc bias. At the expense of reduced bandwidth and increased optical complexity, this power can be reduced to less than a watt by a correct choice of the modulator dimensions (optimum deisgn). In the zigzag configuration, CuCl appears to be slightly better than $SrTiO_3$, in the sense of achieving moderately broadband performance with low modulating power. Cuprous chloride has the advantage of extreme bandwidth, of not requiring any bias, and of not needing reflecting mirrors since θ_i exceeds the critical angle for total reflection. Compared with cavity-type modulators using KDP[35] or ADP[36] the CuCl zigzag modulator typically requires three orders of magnitude less drive power and has up to two orders of magnitude greater bandwidth. Compared with other traveling-wave systems,[3] or with those iterative structures proposed to date,[5] it is substantially superior from the viewpoints of size and power.

As far as the practical realization of these zigzag modulators is concerned, we believe that there are no insurmountable constructional problems. However, it should be noted that at the present time single crystals of suitable cubic electro-optic materials of the required optical quality and size are not readily available. Continuing materials research, however, indicates that this situation should improve.

We should point out that it appears that high dielectric constant centrosymmetric paraelectrics are particularly well suited to the zigzag configuration. This stems from the fact that the dielectric constant of these materials is intermediate between those of conventional dielectrics and those of ferroelectrics, and their quadratic electro-optic effect is large. The dielectric constant is large enough in these materials that the angle required by the synchronism condition is reduced to the smallest practical value. This results in a long optical path in a crystal of modest physical size, and hence in very efficient use of modulating power. The existence of a large quadratic electro-optic effect allows us to obtain a very large effective linear coefficient by using a suitable dc bias. It is of interest to note in this connection that the performance of the $SrTiO_3$ modulator can be improved somewhat by going to lower temperatures.

In closing, we observe that the volume of active material required in the zigzag modulator can be cut in half by using the double-pass arrangement shown in Fig. 9. Here both the light and the modulating signal are reflected from the end of the modulator, with velocity synchronism being maintained for both incident and reflected waves. In this way the physical length of the crystal required to achieve a given electrical length can be halved.

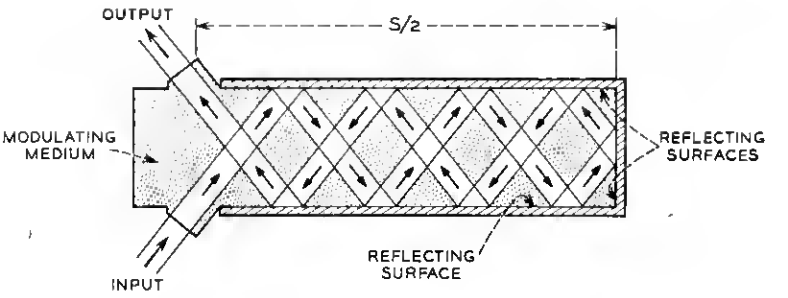

Fig. 9 — Double-pass zigzag modulator configuration.

VIII. ACKNOWLEDGMENTS

We would like to thank L. J. Varnerin, I. P. Kaminow, and E. G. Spencer for critical reading of the manuscript, and for discerning comments.

APPENDIX A

In this appendix we derive expressions for the electric field dependence of the refractive indices of the two normal modes used in the zigzag modulator.

A.1 *Linear Electro-Optic Effect in Cubic Materials of Symmetry T_d*

For this class of materials, to which cuprous chloride belongs, the equation of the index ellipsoid relative to the crystalline axes x',y',z' is[14]

$$\frac{1}{n_0^2}(x'^2 + y'^2 + z'^2) + 2r_{41}(E_{x'}y'z' + E_{y'}z'x' + E_{z'}x'y') = 1 \quad (101)$$

where n_0 is the index of refraction in the absence of the electric fields $E_{x'}$, $E_{y'}$, and $E_{z'}$, and r_{41} is the electro-optic coefficient. For an electric field applied along the z' axis (0° modulator) in a crystallographic [001] direction, the equation reduces to

$$\frac{1}{n_0^2}(x'^2 + y'^2 + z'^2) + 2r_{41}E_{z'}x'y' = 1 \quad (102)$$

which is the equation of an ellipsoid having one of its principal axes along the z' axis, and the remaining two in the $x'y'$ plane at 45° to the x' and

y' axes.* In a coordinate system x,y,z coincident with these axes the index ellipsoid has the normal form

$$\left(\frac{1}{n_0^2} + r_{41}E_z\right)x^2 + \left(\frac{1}{n_0^2} - r_{41}E_z\right)y^2 + \frac{z^2}{n_0^2} = 1. \tag{103}$$

The principal indices of refraction and their respective crystallographic directions are thus

$$\begin{aligned} & & n_x^2 &= \frac{n_0^2}{1 + n_0^2 r_{41} E_z} && \text{along } [110] \\ 0° \text{ case} & & n_y^2 &= \frac{n_0^2}{1 - n_0^2 r_{41} E_z} && \text{along } [\bar{1}10] \\ & & n_z^2 &= n_0^2 && \text{along } [001]. \end{aligned} \tag{104}$$

In the 90° modulator, the field is applied in the x-direction. For this case one principal axis of the index ellipsoid lies along x', and the remaining two in the $y'z'$ plane, at 45° to y' and z'. Again, taking these principal axes as coordinate axes, we find for the principal indices of refraction

$$\begin{aligned} & & n_x^2 &= n_0^2 && \text{along } [100] \\ 90° \text{ case} & & n_y^2 &= \frac{n_0^2}{1 - n_0^2 r_{41} E_x} && \text{along } [011] \\ & & n_z^2 &= \frac{n_0^2}{1 + n_0^2 r_{41} E_x} && \text{along } [0\bar{1}1]. \end{aligned} \tag{105}$$

A.2 *The Quadratic Electro-Optic Effect in Cubic and/or Amorphous Materials*

All substances (solids, liquids, and gases) which have a center of symmetry exhibit the quadratic Kerr effect. For most amorphous substances the electro-optic Kerr effect may be described by the empirical relation[37]

$$\Delta n = K\lambda_0 E^2. \tag{106}$$

In this relation Δn is the induced birefringence, K is the Kerr constant,

* It is not essential that the electric field be applied in a [001] direction. In the general case, however, a principal axis of the index ellipsoid will not be in the direction of the applied field, as we assumed in our analysis in Section II. This complicates both the analysis and operation of the modulator, and results in a decreased electro-optic effect. The basic approach used here would nonetheless remain valid, since for cubic materials the orientation of the index ellipsoid depends only on the *direction* of the applied field, and not on its magnitude. Thus, there is no "wobbling" of the index ellipsoid, and the two normal modes are not mixed in the modulation process.

λ_0 is the free-space optical wavelength, and E is the applied field. Thus in the presence of an electric field isotropic materials effectively become uniaxial and will therefore display the phenomenon of double refraction.

For crystalline solids the effect is more complicated, and must in general be described in terms of a matrix of coefficients. Thus in the general equation for the index ellipsoid

$$a_{11}x'^2 + a_{22}y'^2 + a_{33}z'^2 + 2a_{12}x'y' + 2a_{23}y'z' + 2a_{31}z'x' = 1$$

the coefficients have the field dependence

$$a_{11} - \frac{1}{n_x^2} = \rho_{11}E_{x'}^2 + \rho_{12}E_{y'}^2 + \rho_{13}E_{z'}^2 + \rho_{14}E_{x'}E_{y'} + \rho_{15}E_{y'}E_{z'} + \rho_{16}E_{z'}E_{x'} \quad \text{etc.} \tag{107}$$

leading to a 6×6 matrix of 36 independent electro-optic coefficients ρ_{ij}. As in the linear case, however, crystal symmetry limits the number of nonzero coefficients, and in fact for cubic materials having the highest symmetry (O_h) the quadratic electro-optic effect matrix contains only three independent coefficients and is of the form

$$\rho_{ij} = \begin{bmatrix} \rho_1 & \rho_2 & \rho_2 & 0 & 0 & 0 \\ \rho_2 & \rho_1 & \rho_2 & 0 & 0 & 0 \\ \rho_2 & \rho_1 & \rho_1 & 0 & 0 & 0 \\ 0 & 0 & 0 & \rho_3 & 0 & 0 \\ 0 & 0 & 0 & 0 & \rho_3 & 0 \\ 0 & 0 & 0 & 0 & 0 & \rho_3 \end{bmatrix}. \tag{108}$$

Note that for amorphous materials $\rho_2 = 0$, and $\rho_1 = \rho_3$.

If the field is now applied along a cube edge, e.g., the z' axis of a crystal of symmetry O_h, the equation for the index ellipsoid reduces to

$$\frac{1}{n_0^2}(x'^2 + y'^2 + z'^2) + E_{z'}^2[\rho_2(x'^2 + y'^2) + \rho_1 z'^2] = 1. \tag{109}$$

This equation is in normal form as it stands and shows that the field induces a change in the refractive index isotropically in the $x'y'$ plane as well as along the field direction or z' axis. The principal indices of refraction determined from (109) are

$$n_x^2 = n_y^2 = \frac{n_0^2}{1 + n_0^2\rho_2 E_z^2} \quad \text{along [100], [010]}$$

0° case (110)

$$n_z^2 = \frac{n_0^2}{1 + n_0^2\rho_1 E_z^2} \quad \text{along [001]}.$$

For a field applied in the x direction (90° modulator) the corresponding results are

$$\begin{aligned} n_x^2 &= \frac{n_0^2}{1 + n_0^2 \rho_1 E_x^2} && \text{along [100]} \\ 90° \text{ case} & \qquad\qquad (111) \\ n_y^2 = n_z^2 &= \frac{n_0^2}{1 + n_0^2 \rho_2 E_x^2} && \text{along [010], [001].} \end{aligned}$$

A.3 *Linear Electro-Optic Effect in Uniaxial Materials of Symmetry D_{2d}*

For an electric field applied along the c axis of a uniaxial crystal (taken to be the z' axis, so that we have the 0° case), the equation for the index ellipsoid is[38]

$$\frac{1}{n_0^2}(x'^2 + y'^2) + \frac{1}{n_e^2} z'^2 + 2r_{63}E_{z'}x'y' = 1 \qquad (112)$$

where n_0 and n_e are respectively the ordinary and extraordinary refractive indices, and r_{63} is the electro-optic coefficient of interest. As was the case for cubic materials, one of the principal axes of this ellipsoid lies in the crystallographic [001] direction, the other two in the [110] and [$\bar{1}$10], so that in a coordinate system x,y,z coincident with these axes the principal indices of refraction are

$$\begin{aligned} & n_x^2 = \frac{n_0^2}{1 + n_0^2 r_{63} E_z} && \text{along [110]} \\ 0° \text{ case} \quad & n_y^2 = \frac{n_0^2}{1 - n_0^2 r_{63} E_z} && \text{along [}\bar{1}\text{10]} \qquad (113) \\ & n_z^2 = n_e^2 && \text{along [001].} \end{aligned}$$

For the 90° case the modulating field is still applied along the c axis, but this is taken in the x direction so that the principal indices of refraction are

$$\begin{aligned} & n_x^2 = n_e^2 && \text{along [100]} \\ 90° \text{ case} \quad & n_y^2 = \frac{n_0^2}{1 - n_0^2 r_{63} E_x} && \text{along [011]} \qquad (114) \\ & n_z^2 = \frac{n_0^2}{1 + n_0^2 r_{63} E_x} && \text{along [0}\bar{1}\text{0].} \end{aligned}$$

APPENDIX B

In this appendix we develop some expressions for the output of the three modulator-detector systems enumerated in Section 5.6, using (83) and (84) to account for the effects of random strain. These equations for the wave amplitudes at the output of the modulator were

$$e_{\perp}(\mathbf{r},t) = E_{\perp} \exp \{j[\omega t + \varphi_{\perp}(t)]\} \exp [j\delta_{\perp}(\mathbf{r})] \tag{115}$$

and

$$e_{\parallel}(\mathbf{r},t) = E_{\parallel} \exp \{j[\omega t + \varphi_{\parallel}(t)]\} \exp [j\delta_{\parallel}(\mathbf{r})]. \tag{116}$$

B.1 *Amplitude Modulators*

When the waves given by (115) and (116) are incident on an analyzer whose axes are inclined at an angle θ to $e_{\perp}$, the transmitted wave is

$$e_t(\mathbf{r},t) = e_{\perp}(\mathbf{r},t) \cos \theta + e_{\parallel}(\mathbf{r},t) \sin \theta. \tag{117}$$

The total transmitted power is proportional to

$$\int | e_t(\mathbf{r},t) |^2 da,$$

the integration extending over the beam cross section, and contains the ac terms or information carrying output terms

$$P(t) \mid_{ac} \propto E_{\perp}E_{\parallel} \cos \theta \sin \theta \left[\cos \varphi(t) \int_S \cos \delta(\mathbf{r})\, da - \sin \varphi(t) \int_S \sin \delta(\mathbf{r})\, da \right] \tag{118}$$

where $\varphi(t) = \varphi_{\perp}(t) - \varphi_{\parallel}(t)$ and $\delta(\mathbf{r}) = \delta_{\perp}(\mathbf{r}) - \delta_{\parallel}(\mathbf{r})$.

B.2 *Heterodyne Detection*

In this system we beat in a square-law mixer a phase-modulated signal with a temporally and spatially coherent local oscillator, obtaining an output proportional to the product of the local oscillator and signal amplitudes. For a local oscillator wave of the form

$$e_{LO}(\mathbf{r},t) = E_{LO} \exp [j(\omega_{LO}t + \psi)] \tag{119}$$

the wave amplitude of the output difference frequency is given by

$$e_d(\mathbf{r},t) \propto E_{\perp,\parallel}E_{LO} \cos [(\omega - \omega_{LO})t - \psi + \varphi_{\perp,\parallel}(t) + \delta_{\perp,\parallel}(\mathbf{r})]. \tag{120}$$

This represents the wave amplitude produced at each point on the surface of the mixer. What is of significance beyond this point is the average amplitude $\langle e_d(t)\rangle$, since this determines the response of the IF system.* Averaging over the mixer cross section A_m gives

$$\langle e_d(t)\rangle = E_{\perp,\parallel}E_{\text{LO}}\left\{\cos\left[(\omega-\omega_{\text{LO}})t-\psi+\varphi_{\perp,\parallel}(t)\right]\right.$$
$$\times\frac{1}{A_m}\int_S\cos\delta_{\perp,\parallel}(\mathbf{r})\,da-\sin\left[(\omega-\omega_{\text{LO}})t-\psi\right. \tag{121}$$
$$\left.\left.+\varphi_{\perp,\parallel}(t)\right]\frac{1}{A_m}\int\sin\varphi_{\perp,\parallel}(\mathbf{r})\,da\right\}.$$

B.3 *Phase Modulator and Optical Discriminator*

To be specific, we consider an elementary discriminator formed by operating on the side of the resonance of a Fabry-Perot etalon. If we operate at the half-transmission point, the output wave is to first order given by

$$e_0(\mathbf{r},t) = \tfrac{1}{2}[1+M(\omega_{\text{inst}}-\omega)]e_{\perp,\parallel}(\mathbf{r},t) \tag{122}$$

where M is the slope of the transmission curve at ω, and ω_{inst} is the instantaneous frequency

$$\begin{aligned}\omega_{\text{inst}} &= \frac{\partial}{\partial t}\left[\omega t+\varphi_{\perp,\parallel}(t)+\delta_{\perp,\parallel}(\mathbf{r})\right]\\ &= \omega+\frac{\partial\varphi_{\perp,\parallel}(t)}{\partial t}.\end{aligned} \tag{123}$$

The total transmitted power is proportional to

$$\int|e_0(\mathbf{r},t)|^2\,da,$$

and for small frequency deviations the output power is therefore given by

$$P(t)\propto\left[1+M\frac{\partial\varphi_{\perp,\parallel}(t)}{\partial t}\right]^2E_{\perp,\parallel}{}^2\int_S|\exp\left[j\delta_{\perp,\parallel}(\mathbf{r})\right]|^2\,da. \tag{124}$$

* Regardless of the form of detector (photodiode,[39,40] photoconductor[41] or photoemitter[42,43]) the optical mixing occurs over a finite area large compared with an optical wavelength, but small compared to the different frequency wavelength. Thus we consider that the total difference frequency output of the mixer is a sum of the independent contributions from each elemental portion of the active area, i.e., it is proportional to the value of e_d averaged over the photo surface.

It should be borne in mind that (124) is strictly valid only when the discriminator is illuminated with perfectly collimated light. Strain has the additional complicating effect of producing a spread in the beam incident on the discriminator. Such a distribution of incident angles is equivalent to a broadening of the discriminator frequency response, and hence reduces the FM-to-AM conversion efficiency.

APPENDIX C

The coupling structure analyzed in this appendix is the Fabry-Perot resonator shown schematically in Fig. 10(a). The dimensions of the resonator L_c (length) and l_c (spacing) are both assumed to be much larger than the optical wavelength. The structure can therefore be analyzed in terms of plane waves bouncing back and forth between plates. Since the length of the coupler is finite, we assume that energy

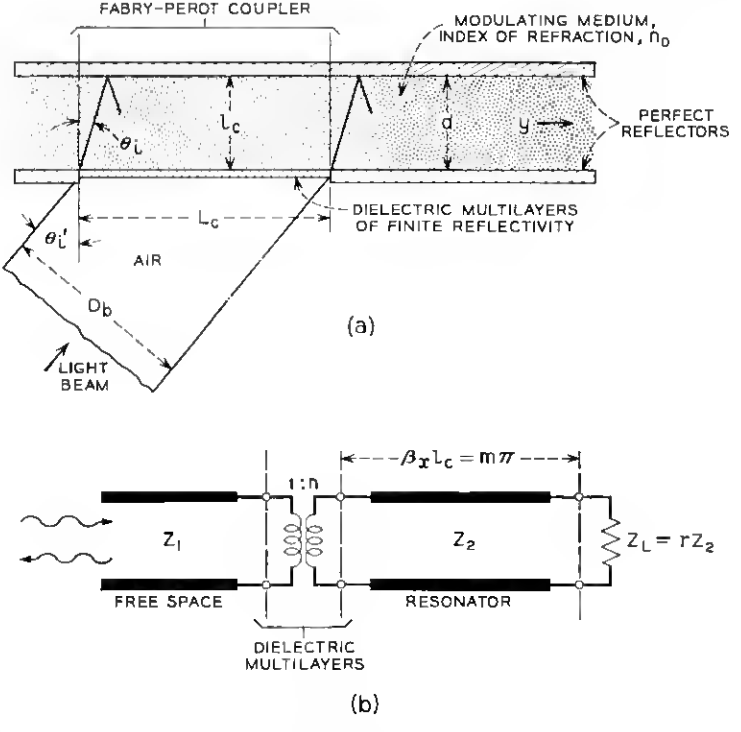

Fig. 10 — Fabry-Perot coupler for optically matching to the modulator when the aperture exceeds the reflector spacing: (a) geometrical arrangement; (b) equivalent circuit.

leaks off to the right in the y direction with group velocity $v_g = (c/n_0) \sin \theta_i'$. Neither diffraction losses nor losses within the electro-optic medium are included in this treatment.

We take as a model for the Fabry-Perot resonator a resonant transmission line system with equivalent circuit shown in Fig. 10(b). The resonator is represented by a transmission line which is an integral number of half wavelengths long in the transverse or x direction. The "walk-off" losses are represented by assigning a small resistance, $Z_L = rZ_2$, to the terminating short circuit. Losses can be introduced in a variety of ways, but for high-Q resonators the results are independent of the way the losses are introduced; for the present treatment the representation chosen is particularly convenient. The finite reflectivity dielectric multilayers are represented by an ideal transformer. Strictly speaking, the transformer turns ratio n will depend upon the angle of incidence and details of the multilayer construction. Experimentally, n is deduced by measuring the reflectivity of the multilayers when the resonator is terminated so as to eliminate reflections from the back surface (i.e., the perfect reflector). Finally, the characteristic impedances Z_1 and Z_2 refer, respectively, to the wave impedances of free space and the electro-optic material in the x direction. They depend upon the index of refraction, angle of incidence, and direction of polarization of the optical signal. In order to illustrate the design principles for such a coupling system, we note that for waves polarized perpendicular to the plane of incidence in Fig. 10(a), Z_1 and Z_2 are given by[9]

$$Z_1 = \eta \sec \theta_i' \tag{125}$$

and

$$Z_2 = \frac{\eta}{n_0} \sec \theta_i \tag{126}$$

where $\eta = 377$ ohms is the intrinsic impedance of free space and n_0 is the refractive index of the modulator material.

The objective of the analysis which is to follow is basically to calculate the dimensions of the Fabry-Perot coupler and the required reflectivity for 100 per cent transmission of light, in terms of known parameters. We begin by observing that for a given aperture D_b the coupler length L_c is given either by

$$L_c = D_b(1 - n_0^2 \sin^2 \theta_i)^{-\frac{1}{2}} \tag{127}$$

where use has been made of Snell's law in relating θ_i to θ_i', or by

$$L_c = D_b/\cos \theta_i . \tag{128}$$

Two equations are required to specify L_c, since it is possible for the angle of incidence required to achieve velocity synchronism to exceed the maximum achievable incident angle Θ_i determined by the limit angle relation

$$\sin \Theta_i = 1/n_0 .$$

It is found in fact that in order to achieve velocity matching the external angle of incidence must satisfy the relation

$$\sin \theta_i' = \frac{n_0^2}{\sqrt{\kappa'}}$$

and for the case $n_0^2 > \sqrt{\kappa'}$, (e.g., CuCl) we cannot employ the arrangement of Fig. 10(a) for which (127) applies. In that case it is necessary to use a more complex coupler such as the one given in Fig. 11 and use (128) in place of (127) to calculate L_c. The spacing l_c can next be found from the resonance condition $\beta_x l_c = m\pi$, which yields

$$l_c = \frac{m\lambda_0}{2n_0 \cos \theta_i}, \qquad \text{for} \quad m = 0, 1, 2, \cdots . \tag{129}$$

The calculation of the requisite reflectivity for 100 per cent light transmission into the modulator can be found in the following manner. We can couple all of the incident energy into the modulator by choosing the turns ratio n (i.e., the reflectivity of the multilayers) to obtain critical coupling, in which case the loaded Q, Q_L, becomes half of the

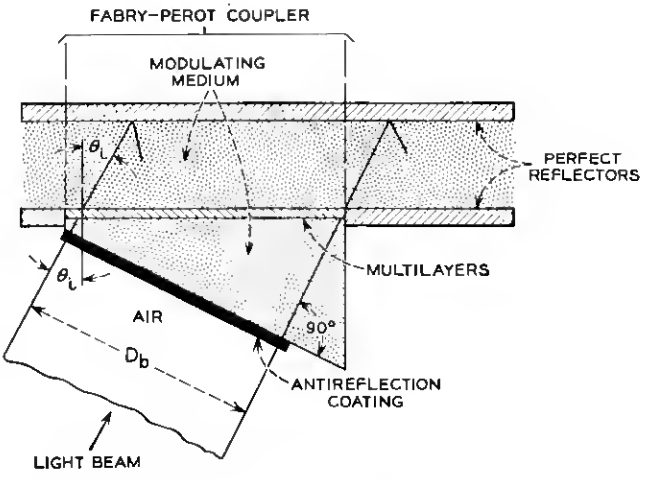

Fig. 11 — Modified coupling arrangement used when $n_0^2/\sqrt{\kappa'} > 1$.

unloaded Q, Q_0, of the resonator. Since the resonator is an integral number of half wavelengths long, the condition for critical coupling is equivalent to choosing n to satisfy the impedance matching relation

$$n^2 = r\frac{Z_2}{Z_1}. \tag{130}$$

Disregarding for the moment the determination of r, which, as will be shown subsequently, can be expressed in terms of the unloaded resonator Q, we find that the multilayer reflectivity, or square of the input reflection coefficient when transmission line Z_2 is terminated [see Fig. 10(b)], must be chosen so that

$$R_c = \left(\frac{1-r}{1+r}\right)^2. \tag{131}$$

Equation (130) has been used in obtaining this result.

There only remains now the problem of determining the dimensionless constant r. The unloaded Q of the resonator can be found by observing that energy must leak off in the y-direction [Fig. 10(a)] with group velocity $v_g = (c/n_0)\sin\theta_i$. The power flow to the right then is

$$P = \frac{W_s}{L_c}v_g$$

where W_s/L_c is the optical energy stored per unit length in the Fabry-Perot, and so the resonator $Q(Q_0 = \omega W_s/P)$ is simply

$$Q_0 = 2\pi\frac{L_c}{\lambda_0}n_0\csc\theta_i. \tag{132}$$

On the other hand, for the equivalent circuit of Fig. 10(b) the unloaded Q is given by

$$Q_0 = m\pi/2r. \tag{133}$$

The constant r can now be found by equating (132) and (133). Then by using (127) or (128) and (129) to eliminate L_c and the integer m, we finally arrive at the formula

$$r = \frac{1}{2}\frac{l_c}{D_b}\sin\theta_i\cos\theta_i\begin{cases}\sqrt{1-n_0^2\sin^2\theta_i} & \text{for } n_0^2 < \sqrt{\kappa'} \\ \cos\theta_i & \text{for } n_0^2 > \sqrt{\kappa'}.\end{cases} \tag{134}$$

It should be noted that the final results drawn from this analysis are valid only when the light is polarized normal to the plane of incidence. The method of analysis outlined applies quite generally, however, and

can be used for any plane of polarization provided that the characteristic impedances Z_1 and Z_2 can be determined. For design purposes the expressions of particular significance are (127), (128) and (129), which fix the dimensions of the coupler, and (131) and (134), which give the necessary reflectivity for transferring 100 per cent of the light into the modulator (neglecting, of course, diffraction losses).

One final comment is in order concerning the output coupler. It is evident almost by inspection that the output coupler could be of precisely the same form as the input coupler but would transmit only half of the light. As an alternative, we suggest using a scheme whereby the beam is simply allowed to diverge at the output of the modulator. If the beam divergence as determined by (49) is not excessive, then in principle all of the light could be collected by a lens, thus making the output coupler 100 per cent efficient.

REFERENCES

1. Rigrod, W. W., and Kaminow, I. P., Wide-Band Microwave Light Modulation, Proc. IEEE, **51**, Jan., 1963, p. 137.
2. Kaminow, I. P., and Liu, J., Propagation Characteristics of Partially Loaded Two-Conductor Transmission Line for Broadband Light Modulators, Proc. IEEE, **51**, Jan., 1963, p. 133.
3. Peters, C. J., Gigacycle Bandwidth Coherent Light Traveling-Wave Phase Modulator, Proc. IEEE, **51**, Jan., 1963, p. 147.
4. Kaminow, I. P., Kompfner, R., and Louisell, W. H., Improvements in Light Modulators of the Traveling-Wave Type, I.R.E. Trans. Microwave Theory and Techniques, **MTT-10**, Sept., 1962, p. 311.
5. White, R. M., and Enderby, C. E., Electro-Optical Modulators Employing Intermittent Interaction, Proc. IEEE, **51**, Jan., 1963, p. 214.
6. See, for instance, Rabinowitz, P., Jacobs, S., Targ, R., and Gould, G., Homodyne Detection of Phase-Modulated Light, Proc. IEEE, **50**, Nov., 1962, p. 2365.
7. Born, M., and Wolf, E., *Principles of Optics*, Pergamon Press, New York, 1959, Chap. XIV.
8. Landau, L. D., and Lifshitz, E. M., *The Classical Theory of Fields*, Addison-Wesley Publishing Co., Inc., Reading, Mass., 1951, Chap. 7.
9. Ramo, S., and Whinnery, J. R., *Fields and Waves in Modern Radio*, second ed., John Wiley and Sons, Inc., New York, 1953, p. 298.
10. Jenkins, F. A., and White, H. E., *Fundamentals of Optics*, McGraw-Hill, New York, 1957, 3rd edition, Sec. 27.4.
11. See Ref. 7, Section 8.5.2.
12. Heavens, O. S., *Optical Properties of Thin Solid Films*, Academic Press, New York, 1955.
13. *American Institute of Physics Handbook*, edited by Gray, D. E., McGraw-Hill, New York, 1957, Sec. 6C.
14. Mason, W. P., Optical Properties and the Electro-Optic and Photoelastic Effects in Crystals Expressed in Tensor Form, B.S.T.J., **29**, April, 1950, p. 161.
15. Harris, S. E., and Siegman, A. E., A Proposed FM Phototube for Demodulating Microwave-Frequency-Modulated Light Signals, I.R.E. Trans. Electron Devices, **ED-9**, July, 1962, p. 322; see also Harris, S. E., Conversion of FM Light to AM Light Using Birefringent Crystals, Appl. Phys. Letters, **2**, Feb., 1963, p. 47.
16. Kaminow, I. P., Splitting of Fabry-Perot Rings by Microwave Modulation of Light, Appl. Phys. Letters, **2**, January, 1963, p. 41.

17. Kanzig, W., *Solid State Physics*, ed. Seitz, F., and Turnbull, D., Academic Press, New York, 1957, pp. 88–91.
18. Pöckels, F., *Lehrbuck Der Kristalloptik*, B. Teubner, Leipzig, 1906.
19. Kaminow, I. P., and Harding, G. O., Complex Dielectric Constant of KH_2PO_4 at 9.2 Gc/sec, Phys. Rev., **129**, Feb., 1963, p. 1562.
20. Landauer, R., Loss Tangent in Ferroelectric Above an Order-Disorder Transition, Bull. Am. Phys. Soc., **8**, Jan., 1963, p. 61.
21. Rupprecht, G., and Bell, R. O., Microwave Losses in Strontium Titanate Above the Phase Transition, Phys. Rev., **125**, March, 1962, p. 1915.
22. Silverman, B. D., Microwave Absorption in Cubic Strontium Titanate, Phys. Rev., **125**, March, 1962, p. 1921.
23. Gordon, E. I., and Rigden, J. D., The Fabry-Perot Electrooptic Modulator, B.S.T.J., **42**, Jan., 1963, p. 155.
24. Hornig, A. W., Doctoral Dissertation, Stanford University, Stanford, California, 1955. Available from University Microfilms, Ann Arbor, Mich., Publ. No. 13,268.
25. Benedict, T. S., and Durand, J. L., Dielectric Properties of Single Domain Crystals of $BaTiO_3$ at Microwave Frequencies, Phys. Rev., **109**, Feb., 1958, p. 1091.
26. Kurtz, S. K., private communication.
27. Bell, R. O., and Rupprecht, G., Measurement of Small Dielectric Losses in Material with a Large Dielectric Constant at Microwave Frequencies, I.R.E. Trans. Microwave Theory and Techniques, **MTT-9**, May, 1961, p. 239.
28. Rupprecht, G., Bell, R. O., and Silverman, B. D., Nonlinearity in Microwave Losses in Cubic Strontium Titanate, Phys. Rev., **123**, July, 1961, p. 97.
29. Geusic, J. E., Kurtz, S. K., Nelson, T. J., and Wemple, S. H., Nonlinear Dielectric Properties of $KTaO_3$ near Its Curie Point, Appl. Phys. Letters, **2**, May 15, 1963, p. 185.
30. West, C. W., Electro-Optic and Related Properties of Crystals with the Zinc Blende Structure, J. Opt. Soc. Am., **43**, April, 1953, p. 335.
31. Sterzer, F., Blattner, D. J., Johnson, H. C., and Miniter, S., 1963 International Solid State Circuits Conf. Digest of Technical Papers, p. 112.
32. Carpenter, R. O'B., The Electro-Optic Effect in Uniaxial Crystals of the Dihydrogen Phosphate Type, J. Opt. Soc. Am., **40**, April, 1950, p. 225.
33. Kaminow, I. P., Paper presented at Quantum Electronics Conference, Paris, February, 1963.
34. See Ref. 17, p. 124.
35. Kaminow, I. P., Microwave Modulation of the Electro-Optic Effect in KH_2PO_4, Phys. Rev. Letters, **6**, May, 1961, p. 528.
36. Blumenthal, R. H., Design of a Microwave Frequency Light Modulator, Proc. I.R.E., **50**, April, 1962, p. 452.
37. Born, M., *Optik*, J. Springer, Berlin, 1933, Chap. 80
38. Billings, B. H., The Electro-Optic Effect in Uniaxial Crystals of the Type $[XH_2PO_4]$, J. Opt. Soc. Am., **39**, Oct., 1949, p. 797.
39. Reisz, R. P., High Speed Semiconductor Photodiodes, Rev. Sci. Instr., **33**, Sept., 1962, p. 994.
40. Anderson, L. K., 1963 International Solid State Circuits Conf. Digest of Technical Papers, p. 114.
41. DiDomenico, M., Jr., Pantell, R. H., Svelto, O., and Weaver, J. N., Optical Frequency Mixing in Bulk Semiconductors, Appl. Phys. Letters, **1**, Dec., 1962, p. 77.
42. McMurtry, B. J., and Siegman, A. E., Photomixing Experiments with a Ruby Optical Maser and Traveling-Wave Microwave Phototube, Appl. Opt., **1**, January, 1962, p. 51.
43. Chemelli, R. G., unpublished work.
44. See Ref. 9, p. 298.